1962

A strip line with variable magnetic film discontinuity

Dinh Tuan Ngo
Iowa State University

A STRIP LINE WITH VARIABLE MAGNETIC FILM DISCONTINUITY

by

Dinh Tuan Ngo

A Dissertation Submitted to the
Graduate Faculty in Partial Fulfillment of
The Requirements for the Degree of
DOCTOR OF PHILOSOPHY

Major Subject: Electrical Engineering

Approved:

Signature was redacted for privacy.

In Charge of Major Work

Signature was redacted for privacy.

Head of Major Department

Signature was redacted for privacy.

Dean of Graduate College

Iowa State University
Of Science and Technology
Ames, Iowa

1962

TABLE OF CONTENTS

I. INTRODUCTION

Magnetic films with their attractive magnetic properties and their physical construction flexibility have been used successfully in computer memories, computer logic circuits, parametric devices and many other applications. The purpose of this investigation was to study in both analytical and experimental detail the behavior of ferromagnetic films one step further on the frequency scale, that is, at microwave frequencies, and to suggest the possibility of device applications at microwave frequencies.

Thin magnetic films can be vacuum deposited on glass substrate in small circles or strips with diameters or widths as small as a fraction of a millimeter and still exhibit to the full extent their magnetic properties. Recently the electroplating technique (1, 2) has almost reached a "perfection" state. This technique allows the control of film thickness, of film composition and hence film coercive and film anisotropy fields. In other words, film properties can be easily controlled by this technique.

The magnetic films available for this investigation were made of nickel-iron alloy of approximately 80 percent nickel and 20 percent iron, commonly referred to as 80-20 permalloy. This type of film has low anisotropy and low magnetostriction coefficients. The above alloy was vacuum deposited on glass substrate of 6 mil thickness in the presence of an external magnetic deposition field of a few hundreds of ampere turns per meter parallel to the plane of the film. With this deposition procedure the atomic structure of the film is ordered in such a manner that

it possesses an uniaxial anisotropy along an axis parallel to the original direction of the deposition field. This direction is frequently referred to as "easy" or "rest" direction of magnetization. Perpendicular to that is the "hard" or "transverse" direction which is also in the plane of the film. When the thickness of the film is less than the dimensions of a normal domain (3-6), there will be very slight possibility to find a domain wall (1-4) existing through such thickness of the film. If a film possessed uniaxial anisotropy, the application of a small magnetic field along the easy direction will bring the film to a single domain.

As mentioned above, the film thickness can be controlled and varied over a wide range. The practical thickness varies from a few hundred angstroms to tens of thousands of angstroms depending upon the application. Since the film plated conductor in the strip line can be made as small as one pleases without altering the magnetic properties, it is advantageous to make use of this construction, for the smaller the conductor, the better the results will be as is pointed out later. Depending upon the characteristic impedance desired, the spacing between the conductors can be varied; here again there will be an optimum condition depending upon the particular device as illustrated in Section III, B. For the moment, it will be assumed that the spacing can be as small as a film thickness or as large as several hundred times the thickness of a practical thick film. Such a strip line can support the TEM wave up to 10^6 megacycles before higher order modes can occur. Before such a frequency can be reached, the skin depth problem will be the limiting factor.

Based on the above reasoning, the wave propagated in the strip line

will be of the principle mode. The transmission line approach can be applied here. The propagation constant of the transmission line will depend on the value of capacitance and inductance per unit length of the strip line. The capacitance of the strip line can be assumed constant. The inductance of the strip line will be made up by the external inductance and the internal inductance which mainly comes from the magnetic films. A control of magnetic film permeability implies a control of internal inductance. The effect of the inductance change of the ferromagnetic film on the propagated wave in the strip line can be regulated and as a consequence, it will be possible to make new microwave frequency devices and to have new techniques to solve old problems such as the anisotropy field H_k of the film, the determination of the Lande splitting factor, and the phenomenological damping constant.

II. INVESTIGATION

A. Analytical Study of the Variable Magnetic Film Discontinuity in the Strip Line

The intrinsic impedance of the strip line as well as the propagation constant are functions of the line capacitance and the line inductance. Since the inductance is directly related to the permeability, the magnetic film susceptibility and permeability will be studied in detail. In evaluating the propagation constant, the problem is attacked by treating the strip line as made up by various media such as brass, air and magnetic films, each with its own dielectric constant and its own permeability. The propagation constant of the principle wave was obtained by solving the boundary problem. Since the permeability of brass is very close to that of air and remains constant with respect to the bias field, the only permeability which will change as function of bias field is that of the magnetic film.

1. Susceptibility of the magnetic thin film as a function of bias field

a. Derivation of film susceptibility The torque $\bar{T}$ acting on a unit volume is related to the angular momentum density $\bar{L}$ by

$$\bar{T} = \frac{d\bar{L}}{dt} \qquad 1$$

The magnetization $\bar{M}$ can be written as a function of the angular momentum density as:

$$\bar{M} = \gamma\bar{L} \qquad 2$$

where γ is the gyromagnetic (or magneto-mechanical) ratio and is equal to $\frac{ge\mu_o}{2m}$ for MKS system of units. In this expression g is the Lande splitting factor, e is the electron charge in coulombs, μ_o equals $4\pi \times 10^{-7}$ henry per meter and m is mass of the electron in kg. Numerically $\gamma = 2.21 \times 10^5$ cycles per second per ampere-turn per meter for electron spins. The equation of motion can then be written:

$$\frac{d\bar{L}}{dt} = \bar{M} \times \bar{H} \qquad 3$$

It is important to note that $\bar{H}$ must contain all of the effective fields (forces) which produce torque on the magnetization per unit volume.

Up to this point, it is worthwhile to mention briefly all of the types of fields or the types of energies which are of practical concern. Kittel and others (3, 4) list four types of energy that are of importance in determining domain structure: exchange energy, anisotropy energy, magnetoelastic energy, magnetostatic energy. The lost energy due to viscous damping is taken into consideration in this study. In 80-20 permalloy film, the magnetoelastic energy can be considered negligible due to its low magnetostriction coefficient. The exchange energy is considered for the most part from interaction of electron spins. Since in a perfect single domain ferromagnetic structure, domain rotation is the only mechanism which allows magnetic change to occur, the exchange energy is a constant independent of the magnetization orientation with respect to crystallographic axis. This leaves only the anisotropy and the magnetostatic energy as the major energy contribution in this case of single domain 80-20 permalloy films.

The uniaxial anisotropy energy is given as

$$W_a = K \sin^2 \theta$$

where θ is shown in Figure 1. The magnetostatic energy results from the applied and demagnetizing field. Hence the total field would include external applied field $\bar{H}_e$, the internal anisotropy field $\bar{H}_a$, the demagnetizing field $\bar{H}_d$ and another new field, the dynamic damping loss field $\bar{H}_v$, which takes care of the lost energy (7). This formulation is based on Landau and Lifshitz phenomenological theory of rotational process.

If energy is lost, it must by definition occur from forces opposing the motion. For simplicity, it is assumed that the loss forces are viscous in nature, that is $\bar{H}_v = - \frac{a\dot{\bar{M}}}{\gamma M}$ when a is the phenomenological damping constant and M is the magnitude of the magnetization. Equation 3 then can be written as:

$$\dot{\bar{M}} = \gamma \bar{M} \times (\bar{H} - \frac{a}{\gamma} \frac{\dot{\bar{M}}}{M}) \qquad 4$$

Forming the vector cross product of $\bar{M}$ and Equation 4, one gets:

$$\bar{M} \times \dot{\bar{M}} = \gamma \bar{M} \times \bar{M} \times \bar{H} - \frac{a}{M} \bar{M} \times (\bar{M} \times \dot{\bar{M}}) \qquad 5$$

Since

$$\bar{M} \times (\bar{M} \times \dot{\bar{M}}) = \bar{M} (\bar{M} \cdot \dot{\bar{M}}) - \dot{\bar{M}} (M)^2$$

where the term involving $(\bar{M} \cdot \dot{\bar{M}})$ drops out, Equation 5 can be written in this form:

$$a\dot{\bar{M}} = - \frac{a\gamma}{M} \bar{M} \times (\bar{M} \times \bar{H}) + \frac{a}{M} \bar{M} \times \dot{\bar{M}} \qquad 6$$

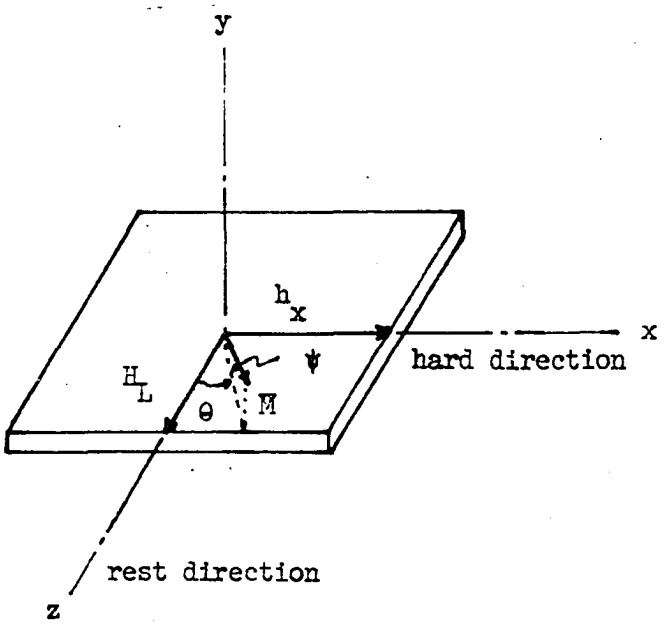

Figure 1. Schematic representations of a single domain thin film with external applied fields

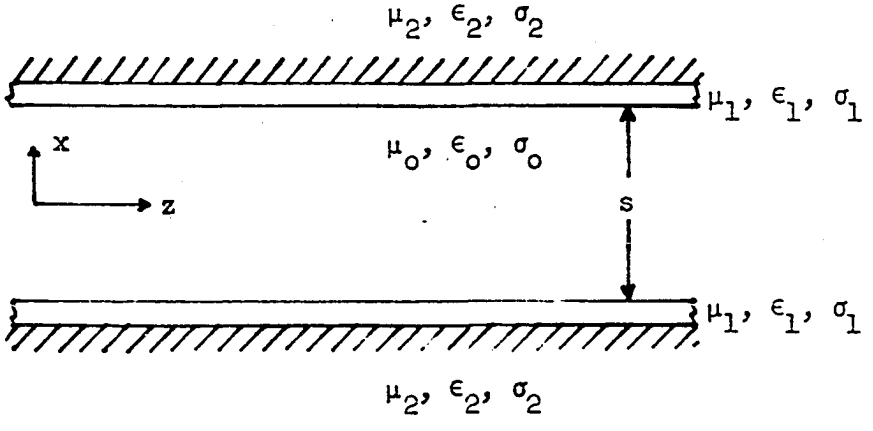

Figure 2. Model for mathematical solutions for waves between permalloy plated imperfectly conducting planes

From Equation 4,

$$\frac{a}{M}\,\bar{M} \times \dot{\bar{M}} = -\dot{\bar{M}} + \gamma \bar{M} \times \bar{H}$$

Substitution in Equation 6 and rearrangement gives:

$$\dot{\bar{M}} = \frac{\gamma \bar{M} \times \bar{H}}{1 + a^2} - \frac{a\gamma}{(1 + a^2)M}\,\bar{M} \times (\bar{M} \times \bar{H}) \qquad 7$$

which is the Landau-Lifshitz form.

The strip line is operated at microwave frequency, the bias field varies over a wide range, and the region of great interest is around resonance, i.e., at high bias field. The phenomenological damping constant a can be assumed to be about 0.01. Equation 7 can be reduced to:

$$M\dot{\bar{M}} = M\gamma \bar{M} \times \bar{H} - a\gamma \bar{M} \times (\bar{M} \times \bar{H}) \qquad 8$$

Consider the magnetic film of a rectangular shape with the coordinates chosen as shown in Figure 1. In the MKS system, the vector magnetic flux density $\bar{B}$ in a magnetic domain is given as:

$$\bar{B} = \mu_o \bar{H} + \bar{M} \qquad 9$$

where μ_o is the permeability of free space, $\bar{H}$ is the total magnetic field intensity at the point of interest, $\bar{M}$ is the vector saturation magnetization per unit volume of material. Since there is no field applied in the y direction, Equation 9 gives the demagnetizing field in the y direction as:

$$h_y = -\frac{m_y}{\mu_o} \qquad 10$$

The easy direction of the film is shown in Figure 1 along the z-axis. The r.f. field is applied along the x-axis and the bias field is applied along the z-axis, as shown in Figure 1.

Writing the magnetization vector $\bar{M}$ in terms of its rectangular components, by noting that the r.f. component of $\bar{M}$ in the z-direction is much less than M_z, induced by the applied bias field, then

$$\bar{M} = \bar{i}m_x + \bar{j}m_y + \bar{k}M_z \qquad 11$$

where $\bar{i}$, $\bar{j}$, and $\bar{k}$ are unit vectors. Similarly $\bar{H}_T$, the total magnetic field intensity can be expressed as:

$$\bar{H}_T = \bar{i}h_x - \bar{j}\frac{m_y}{\mu_o} - \bar{k}(H_L + H_K) \qquad 12$$

where h_x is the r.f. field intensity, $-\frac{m_y}{\mu_o}$ is the demagnetizing field intensity, H_L is the applied field intensity and H_K is the anisotropy field intensity.

Due to dependence upon both time and space, it is to be understood that m_x, m_y and h_x are no more than abbreviated expressions for $m_x e^{j(\omega t - kz)}$, $m_y e^{j(\omega t - kz)}$ and $h_x e^{j(\omega t - kz)}$, respectively.

Making use of Equations 11 and 12,

$$\begin{aligned}\bar{M} \times \bar{H}_T = {} & \bar{i}[m_y(H_L + H_K) + \frac{M_z}{\mu_o} m_y]m_y \\ & + \bar{j}[M_z h_x - m_x(H_L + H_K)] \\ & + \bar{k}[-\frac{m_x m_y}{\mu_o} - m_y h_x]\end{aligned} \qquad 13$$

By assuming small angle or rotation, M_z may be approximated by M and the

product of small quantities may be neglected. For the uniaxial single domain film used, M equals approximately 1 weber/m^2, H_k = 240 ampere-turns/meter, H_L can be assumed of the same order of magnitude; hence $H_L + H_K \ll \frac{M_z}{\mu_o}$.

Equation 13 then reduces to:

$$\bar{M} \times \bar{H}_T = \bar{i}\left(\frac{M_z}{\mu_o}\right)m_y + \bar{j}(M_z h_x - m_x H_o) \qquad 14$$

where

$$H_o = H_L + H_K \qquad 15$$

Substitution of Equation 14 in $\bar{M} \times (\bar{M} \times \bar{H}_T)$ gives

$$\begin{aligned} \bar{M} \times (\bar{M} \times \bar{H}_T) = {} & \bar{i}[-M_z(M_z h_x - m_x H_o)] \\ & + \bar{j}\left[\frac{M_z^2}{\mu_o} m_y\right] \\ & + \bar{k}\left[m_y(M_z h_x - m_x H_o) - \frac{M_z}{\mu_o} m_y^2\right] \end{aligned} \qquad 16$$

Substitution of Equations 13 and 16 into Equation 7 produces the following set of equations:

$$M j\omega m_x = \frac{\gamma M M_z}{\mu_o} m_y + a\gamma M_z (M_z h_x - m_x H_o) \qquad 17$$

$$M j\omega m_y = \gamma M[M_z h_x - m_x H_o] - \frac{a\gamma M_z^2}{\mu_o} m_y \qquad 18$$

$$0 = -a\gamma\left[m_x(M_z h_x - m_x H_o) - \frac{M_z}{\mu_o} m_y^2\right] \qquad 19$$

Maxwell's equation may now be applied to the film medium. The field

equations needed are:

$$\nabla \times \bar{E} = - \frac{\partial \bar{B}}{\partial t} \qquad 20$$

$$\nabla \times \bar{H} = \sigma \bar{E} + \frac{\partial \bar{D}}{\partial t} \qquad 21$$

Permalloy film is a good conductor; hence the displacement current term may be neglected in the above equation, and

$$\nabla \cdot \bar{B} = 0 \qquad 22$$

Taking the curl of Equation 21

$$\nabla \times \nabla \times \bar{H} = \sigma \nabla \times \bar{E} \qquad 23$$

Expanding,

$$\nabla(\nabla \cdot H) - \nabla^2 \bar{H} = - \frac{\sigma \partial}{\partial t} (\mu_o \bar{H} + \bar{M})$$

Since $\nabla \cdot \bar{B} = 0$ from Equation 22,

$$\nabla^2 H = \sigma(\mu_o \frac{\partial \bar{H}}{\partial t} + \frac{\partial \bar{M}}{\partial t}) \qquad 24$$

Recalling that h_x, h_y, m_x and m_y are written with the assumed function $e^{j(\omega t - kz)}$, the x-component of Equation 24 then becomes:

$$-k^2 h_x = j\sigma\omega\mu_o (h_x + \frac{m_x}{\mu_o}) \qquad 25$$

Rearranging Equation 20,

$$(j\sigma\omega\mu_o + k^2)h_x = -j\sigma \mu_o \frac{m_x}{\mu_o} \qquad 26$$

Rearrangement of Equations 17, 18 and 26 with the unknowns in the order

h_x, m_x and m_y,

$$a\gamma M_z^2 h_x - (j\omega M + a\gamma M_z H_o)m_x + a\frac{MM_z}{\mu_o} m_y = 0 \qquad 27$$

$$\gamma MM_z h_x - \gamma MH_o m_x - (j\omega M + a\gamma \frac{M_z^2}{\mu_o})m_y = 0 \qquad 28$$

$$(j\sigma\omega\mu_o + k^2)h_x + j\sigma\omega\, m_x = 0 \qquad 29$$

Non-trivial solutions to Equations 27, 28 and 29 will result if the determinant of the set is zero.

$$\begin{vmatrix} a\gamma M_z^2 & -(j\omega M + a\gamma MH_o) & \frac{\gamma MM_z}{\mu_o} \\ \gamma MM_z & -\gamma MH_o & -(j\omega M + a\gamma \frac{M_z^2}{\mu_o}) \\ (j\sigma\omega\mu_o + k^2) & j\sigma\omega & 0 \end{vmatrix} = 0 \qquad 30$$

Going through with the algebraic manipulation, and neglecting relatively small terms,

$$(j\sigma\omega\mu_o + k^2)(\omega_o^2 - \omega^2 + ja\gamma \frac{M_z}{\mu_o}\omega) = -j\frac{M_z}{\mu_o}\gamma\sigma\omega\mu_o(\frac{M\gamma}{\mu_o} + ja\omega) \qquad 31$$

where

$$\omega_o^2 = \gamma \frac{M}{\mu_o} H_o \qquad 32$$

From Equation 26, the susceptibility χ_x is given by definition as

$$\chi_x = \frac{m_x}{h_x}$$

or

$$\chi_x = \frac{j\sigma\omega\mu_o + k^2}{-j\,\sigma\,\omega} \qquad 33$$

Substituting Equation 31 into Equation 33, one obtains

$$\chi_x = \frac{\gamma M_z \left(\gamma\frac{M}{\mu_o} + ja\omega\right)}{\left[\omega_o^2 - \omega^2 + ja\gamma\frac{M_z}{\mu_o}\omega\right]} \qquad 34$$

If the phenomenological damping constant a is neglected, Equation 32 illustrating the resonant condition will reduce to Equation 20 given by Kittel (8) describing resonance for a plane specimen. Kittel's Equation 20 given in the cgs system of units is:

$$\omega_o = \gamma\left\{(H_z + 4\pi M + \frac{2k_1'}{M_z})(H_z + \frac{2k_1'}{M_z})\right\}^{1/2}$$

where $H_z + \frac{2k'}{M_z}$ is equivalent to H_o in our Equation 32. Since

$$H_z + \frac{2k_1'}{M_z} \ll 4\pi M$$

for the practical purpose, the Kittel's Equation 20 bears the same form as Equation 31 with the term involving the phenomenological constant neglected, namely

$$\omega_o = \gamma\left[4\pi M(H_z + \frac{2k_1'}{M_z})\right]^{1/2}$$

Ferromagnetic resonance phenomena have been investigated from radio frequency to uhf and for different bias configurations (9-14), in the endeavor to study the reversal phenomena, to determine the phenomenological

damping constant a, the anisotropy field, H_k and the Lande splitting factor g. A comparison between these techniques and the methods suggested here will be drawn in Section III, A.

The film permeability may be found from the susceptibility equation. Let

$$\chi_{1x} = \chi'_{1x} - j\chi''_{1x} \tag{35}$$

Rationalization of Equation 34 and recognition that $M_z \cong M$ for small angles results in:

$$\chi_{1x} = \frac{\gamma M(\frac{\gamma M}{\mu_o} + ja\omega)[(\omega_o^2 - \omega^2) - ja\gamma \frac{M}{\mu_o}\omega]}{[(\omega_o^2 - \omega^2)^2 + (a\gamma \frac{M}{\mu_o}\omega)^2]} \tag{36}$$

By noting that $a^2 \ll 1$, the components of χ_{1x} can be presented in a more simple form.

$$\chi'_{1x} = \frac{(\gamma M)^2}{\mu_o} \quad \frac{(\omega_o^2 - \omega^2)}{[(\omega_o^2 - \omega^2)^2 + (\frac{a\gamma M}{\mu_o}\omega)^2]} \tag{37}$$

Similarly, by remembering that $H_o \ll \frac{M}{\mu_o}$, χ''_{1x} can be expressed as:

$$\chi''_{1x} = \frac{a\gamma M\omega(\omega^2 + \frac{\gamma^2 M^2}{\mu_o^2})}{[(\omega_o^2 - \omega^2)^2 + (a\frac{\gamma M}{\mu_o}\omega)^2]} \tag{38}$$

b. <u>The bias field for peak value of the real part of the film susceptibility</u> At this point, it is worthwhile to find the expressions for H_L which will yield peak values of χ'_{1x}.

Substitution of Equations 15 and 32 into Equation 37 gives:

$$\chi'_{1x} = \frac{(\frac{\gamma M}{\mu_o})^2 [\gamma^2 \frac{M}{\mu_o} (H_L + H_K) - \omega_1^2]}{[(\gamma^2 \frac{M}{\mu_o} (H_L + H_K) - \omega_1^2)^2 + (\alpha\gamma \frac{M}{\mu_o} \omega)^2]} \qquad 39$$

where ω_1 is the operating angular velocity. Differention of Equation 39 with respect to H_L and subsequent equating to zero gives:

$$[\gamma^2 \frac{M}{\mu_o} (H_L + H_K) - \omega_1^2] = \pm(\alpha\gamma \frac{M}{\mu_o} \omega_1) \qquad 40$$

With a little arrangement, Equation 40 becomes:

$$H_L = H_{Lo} \pm \frac{a\omega_1}{\gamma} \qquad 41$$

where $H_{Lo} = H_o - H_K$, the value of applied field necessary for resonance. From Equation 41,

$$\Delta H_L = \frac{a\omega_1}{\gamma} \qquad 42$$

Equation 42 agrees with the result given by Conger and Essig (10). Based on Equation 41, it is obvious from Equation 39 that χ'_{1x} will reach its negative peak value at $H_L = H_{Lo} - \frac{a\omega_1}{\gamma}$ and a positive peak value at $H_L = H_{Lo} + \frac{a\omega_1}{\gamma}$.

2. The permeability of magnetic-thin film as a function of bias field.

a. Derivation of magnetic film permeability As mentioned before, the magnetic film flux density in a ferromagnetic domain in the MKS system of units is:

$$\overline{B} = \mu_o \overline{H} + \overline{M}$$

By definition, the permeability is

$$\mu = \frac{B}{H}$$

hence

$$\mu = \mu_o + \chi \qquad 43$$

Since χ_{lx} is shown to be a complex number, similarly μ_{lx} can be written in the same form:

$$\mu_{lx} = \mu'_{lx} - j\mu''_{lx} \qquad 44$$

Since μ_o is the permeability of air, a real number, μ_{lx} then can be written as:

$$\mu'_{lx} = \mu_o + \chi'_{lx} \qquad 45$$

In the situation under investigation here,

$$\mu'_{lx} = \frac{\mu_o(\omega_o^2 - \omega^2)^2 + \mu_o(a\gamma\frac{M}{\mu_o}\omega)^2 + (\frac{\gamma M}{\mu_o})^2(\omega_o^2 - \omega^2)}{[(\omega_o^2 - \omega^2)^2 + (a\gamma\frac{M}{\mu_o}\omega)^2]} \qquad 46$$

Since $\frac{M}{\mu_o} \gg H_o$ and $1 \gg a^2$, Equation 46 becomes, after minor rearrangement:

$$\mu'_{lx} = \frac{\mu_o(\omega_o^2 - \omega^2)\,[(\frac{\gamma M}{\mu_o})^2 - \omega^2]}{[(\omega_o^2 - \omega^2)^2 + (a\gamma\frac{M}{\mu_o}\omega)^2]} \qquad 47$$

From Equation 47 it is observed that μ'_{lx} changes sign twice, one time at resonance, the other at $\omega = \frac{\gamma M}{\mu_o}$. The imaginary part of μ_{lx} is the same as the imaginary part of χ_{lx}, hence:

$$\mu''_{lx} = \frac{\mu_o(a\gamma\frac{M}{\mu_o}\omega)[(\frac{\gamma M}{\mu_o})^2 + \omega^2]}{[(\omega_o{}^2 - \omega^2)^2 + (a\gamma\frac{M}{\mu_o}\omega)^2]} \qquad 48$$

From Equations 47 and 48, it is seen that μ_{lx} will have the following form:

$$\mu_{lx} = \mu_o\mu_{rlx} \qquad 49$$

where μ_{rlx} is the relative permeability. Hence

$$\mu_{rlx} = \frac{(\omega_o{}^2 - \omega^2)[(\frac{\gamma M}{\mu_o})^2 - \omega^2]}{[(\omega_o{}^2 - \omega^2)^2 + (a\frac{\gamma M}{\mu_o}\omega)^2]} - \frac{-j(a\gamma\frac{M}{\mu_o}\omega)[(\frac{\gamma M}{\mu_o})^2 + \omega^2]}{[(\omega_o{}^2 - \omega^2)^2 + (a\frac{\gamma M}{\mu_o}\omega)^2]} \qquad 50$$

b. Peak values of μ_{rlx} Since it is expected that the film permeability will have a direct effect on the behavior of the electromagnetic field in the strip line, it is worthwhile to analyze the permeability curve in detail. Once the relationship between the propagated wave and the film permeability is established, one can be used to predict the behavior of the other, and vice versa.

From Equation 40 it is noted that χ'_{lx} reaches a negative peak value, then a positive peak value; hence it is expected that μ'_{rlx} will behave likewise.

By substituting the negative root of Equation 40 into the real part

of Equation 50 and by making use of the relation $\frac{M}{\mu_o} \gg H_o$, with some arrangement, one obtains

$$\mu'_{rlxMin} = - \frac{\gamma M}{2\mu_o a\omega_1} \qquad 51a$$

Doing likewise with the positive root of Equation 40 one obtains:

$$\mu'_{rlxMax} = \frac{\gamma M}{2\mu_o a\omega} \qquad 51b$$

Equations 51a and 51b offer some interesting information concerning the frequency range at which thin film devices can be operated. Since μ'_{rlx} varies inversely as the operating angular velocity, the higher the frequency, the lower the amplitude of μ'_{rlx}. The saving factor for this situation is that μ'_{rlx} also varies inversely with respect to the damping constant a, which is expected to decrease at high bias field intensities. μ'_{rlx} will go through zero at resonance and at $\omega = \frac{\gamma M}{\mu_o}$.

It is obvious from Equation 50, that μ''_{rlx} will reach a maximum value at resonance, i.e., $\omega^2 = \omega_o^2$. By substituting this relation into the imaginary part of Equation 50, and taking into consideration the fact $\frac{M}{\mu_o} \gg H_o$,

$$\mu''_{rlxMax} \quad \frac{\gamma M}{\mu_o a\omega} \quad . \qquad 52$$

Comparison of Equation 52 with Equation 51b,

$$\mu''_{rlxMax} = 2\mu'_{rlxMax} \qquad 53$$

It is interesting to note from Equation 53 that the maximum of the real

part of μ_{rlx} is related to the maximum of the imaginary part of μ_{rlx} by a factor 1/2.

It is informative to find the value of μ''_{rlx} at the bias field intensity H_p, where μ''_{rlx} reaches the peak value. By substituting Equation 30 into the imaginary part of μ_{rlx} and making use of the relation $\frac{M}{\mu_o} \gg H_o$, one gets

$$\mu''_{rlx}\Big|_{H_p} = \frac{\gamma M}{2a\mu_o\omega} \qquad 54$$

Hence

$$\mu''_{rlx}\Big|_{H_p} = \mu'_{rlxMax} \qquad 55$$

From Equation 55 it is observed that the peaks of the real part of μ_{rlx} will occur right at the half width position of the imaginary part of μ_{rlx} and equal half of its maximum value. The amplitude of μ''_{rlx} also varies inversely with angular velocity ω and damping constant a.

In summary the magnetic film permeability is made up of a real part which contributes the inductance to the line and the imaginary part which represents the loss component. The real part varies from a negative value, reaches a negative peak, goes through zero then reaches a positive peak as the bias field increases; while the imaginary part representing the power absorption of the film at resonance always remains positive and reaches a peak at resonance bias field intensity. The peak value of the real part is related to that of the imaginary part by a factor 1/2

and occurs at the half width points of the latter.

3. The boundary value problem

Before solving the boundary value problem, a discussion of the following assumption will be in order.

The conductivity of a permalloy film is in the neighborhood of one tenth of that of copper, and its skin depth at 1000 Mc is about 6 x 10^{-4} cm or 60,000 angstroms. The practical film thickness varies from 50 to 5000 angstroms depending on the application. The film used for the investigation was approximately two thousand angstroms thick. The ratio between the film thickness of 2000 angstroms and the skin depth is about 3.3%. Under these circumstances,

$$H = H_o e^{-0.033} e^{-j0.033} = 0.97 H_o e^{-j0.033}$$

The amplitude and the phase constant change about three per cent throughout the film thickness. It is reasonable to assume that for a film not much thicker than 2000 angstroms and with the operating frequency around 1000 Mc, the magnitude and phase of the electromagnetic wave remain the same through the film thickness and as a consequence, for the above operating frequency, the spin wave effect may be neglected, (15, 16). For thinner films, the frequency may be much higher and the above assumption is still satisfied. With that assumption, the boundary value problem can be attacked directly.

Consider two parallel planes made up by a good conductor coated with a magnetic thin film as shown in Figure 2. Let air be designated as medium 0, permalloy film as medium 1, and the outside conductor as

medium 2. Starting with Maxwell's equations

$$\nabla \cdot \bar{D} = 0 \tag{56}$$

$$\nabla \cdot \bar{B} = 0 \tag{57}$$

$$\nabla \times \bar{E} = -\frac{\partial \bar{B}}{\partial t} \tag{58}$$

$$\nabla \times \bar{H} = \sigma \bar{E} + \frac{\partial \bar{D}}{\partial t} \tag{59}$$

Forming the curl of Equation 58,

$$\nabla \times \nabla \times \bar{E} = -\mu \quad \nabla \times \frac{\partial \bar{H}}{\partial t} \quad .$$

Expanding,

$$\nabla(\nabla \cdot \bar{E}) - \nabla^2 \bar{E} = -\mu \quad \nabla \times \left(\frac{\partial \bar{H}}{\partial t}\right)$$

By remembering that $\nabla \cdot \bar{E} = 0$ from Equation 56 and that time and space partial derivatives may be taken in either order, and obtaining $\nabla \times \bar{H}$ from Equation 59, one finds:

$$\nabla^2 \bar{E} = -\frac{\partial}{\partial t}\left(\sigma \bar{E} + \epsilon \frac{\partial}{\partial t} \bar{E}\right) \tag{60}$$

where σ is the conductivity.

In all analysis to follow, all the coefficients E_x, H_x, E_y, etc. are functions of x and y only; since the z and time functions are taken care of in the assumed $e^{j\omega t - \Gamma z}$. Hence

$$\nabla^2 \bar{E} = \nabla_{xy}^2 \bar{E} + \frac{\partial^2}{\partial z^2} \bar{E}$$

and

$$\frac{\partial^2 E}{\partial z^2} = \Gamma^2 E$$

Equation 60 then can be written as

$$\nabla_{xy}^2 \bar{E} + \Gamma^2 \bar{E} = j\omega\mu (\sigma + j\omega\epsilon) \bar{E}$$

Assuming there is no variation in the y-direction, the above equation reduces to

$$\frac{d^2 E}{dx^2} = -k^2 \bar{E} \qquad 61$$

where

$$k^2 = \Gamma^2 - j\omega\mu(\sigma + j\omega\epsilon) \qquad 62$$

a. Medium 0: air Since in free space, $\sigma_o \ll \omega\epsilon_1$, one has

$$k_o^2 = \Gamma^2 + \omega^2 \mu_o \epsilon_o \qquad 63$$

Due to the boundary condition involved a solution with E_z odd in x is sought and expressed as a sine term.

$$E_{zo} = A_o \text{ Sin } K_{ox} \qquad 64$$

From (17)

$$E_x = - \frac{1}{\Gamma^2 + k^2} \left[\frac{\partial E_z}{\partial x} + j\omega\mu \frac{\partial H_z}{\partial y} \right]$$

where $k^2 = \omega^2 \mu \epsilon$

$$E_x = - \frac{\Gamma}{k_o} A \text{ Cos } K_o x \qquad 65$$

H_y is given from (17) as:

$$H_y = - \frac{1}{\Gamma^2 + k^2} \left[j\omega\epsilon \frac{\partial E_z}{\partial x} + \gamma \frac{\partial H_z}{\partial y} \right]$$

Since $H_z = 0$,

$$H_y = \frac{-j\omega\epsilon_o}{k_o} A_o \text{ Cos } k_o x \qquad 66$$

b. Medium 1: permalloy film From this point on, the subscript x on the magnetic film permeability μ_1 is dropped to simplify the equations.

Let the permeability, the conductivity and the dielectric constant of permalloy film be designated as μ_1, σ_1 and ϵ_1 respectively. For conducting magnetic film, it follows that

$$\nabla^2_{xy} E = -(\Gamma^2 + k^2) E$$

using the same Γ as in the free space region, since the continuity relations between the fields of the two regions must be satisfied at the boundary for all values of z. Assuming that there is no variation in the y-direction, one has:

$$\frac{d^2 E_z}{dx^2} = -k_1^2 E_z \qquad 67$$

where

$$k_1^2 = \Gamma^2 - j\omega\mu_1(\sigma_1 + j\omega\epsilon_1)$$

Since permalloy film is a good conductor, then this relation $\sigma_1 \gg \mu_1\epsilon_1$ holds, and the following equation results:

$$k_1^2 = \Gamma^2 - j\omega\mu_1\sigma_1 \qquad 68$$

E_{z1} then has the solution of the form:

$$E_{z1} = B_1 e^{-jk_1 x} + B_2 e^{jk_1 x} \qquad 69$$

Referring to the continuity relation at the boundary mentioned above, since Γ^2 should turn out to be of the same order of magnitude as $\omega^2\mu_o\epsilon_o$, and since $\frac{\omega\epsilon_1}{\sigma_1} \ll 1$, Γ in Equation 68 may be neglected; hence

$$k_1^2 = -j\omega\mu_1\sigma_1 \qquad 70$$

Carrying out the same procedure as in free space, one finds:

$$E_{x1} = \frac{j\Gamma}{k_1}\left[B_1 e^{-jk_1 x} - B_2 e^{jk_1 x}\right] \qquad 71$$

Similarly

$$H_{y1} = \frac{j\sigma_1}{k_1}\left[B_1 e^{-jk_1 x} - B_2 e^{jk_1 x}\right] \qquad 72$$

At the boundary, i.e., at $x = \frac{s}{2}$, E_z and H_y must be continuous. Applying the boundary condition to the tangential electric field in Equation 64 and Equation 69, one obtains

$$A_o \operatorname{Sin} k_o \frac{s}{2} = B_1 e^{-jk_1\frac{s}{2}} + B_2 e^{jk_1\frac{s}{2}} \qquad 73$$

Application of the boundary condition to the tangential magnetic field in Equation 66 and Equation 72 gives:

$$-\frac{\omega\epsilon_o}{k_o} A_o \operatorname{Cos} k_o \frac{s}{2} = \frac{\sigma_1}{k_1} \left[B_1 e^{-jk_1 \frac{s}{2}} - B_2 e^{jk_1 \frac{s}{2}}\right] \qquad 74$$

c. Medium 2: the conducting material For the conducting material in region 2, using the same Γ as in region 1, i.e., the same Γ as in free space due to the continuity relation for all z one may also write

$$\frac{d^2 E_z}{dx^2} = -k_2^2 E_z \qquad 75$$

where

$$k_2^2 = \Gamma^2 - j\omega\mu_2(\sigma_2 + j\omega\epsilon_2) \qquad 76$$

Since medium 2 is made up of good conducting material, the $j\omega\epsilon_2$ term as well as Γ^2 may be neglected, with the approximate result:

$$k_2^2 = -j\omega\mu_2\sigma_2 \qquad 77$$

The solution of Equation 75 is written in terms of exponentials, retaining only the negative exponential term so that the field intensity will die off properly as x approaches infinity. The result is:

$$E_{z2} = C_2 e^{-jk_2 x} \qquad 78$$

For the electric field and the magnetic field in this region,

carrying out the same procedure as for the two previous media and using the condition mentioned above, one gets:

$$E_{x2} = \frac{j\Gamma}{k_2} C_2 e^{-jk_2 x} \qquad 79$$

$$H_{y2} = \frac{j(\sigma_2)}{k_2} C_2 e^{-jk_2 x} \qquad 80$$

Let

$$s + 2d = b \qquad 81$$

where d is the magnetic film thickness.

Applying the boundary condition to the electric field in Equations 69 and 78,

$$B_1 e^{-jk_1 \frac{b}{2}} + B_2 e^{jk_1 \frac{b}{2}} = C_2 e^{-jk_2 \frac{b}{2}} \qquad 82$$

Doing likewise for the magnetic field in Equations 72 and 80,

$$\frac{\sigma_1}{k_1}\left[B_1 e^{-jk_1 \frac{b}{2}} - B_2 e^{jk_1 \frac{b}{2}}\right] = \frac{\sigma_2}{k_2} C_2 e^{-jk_2 \frac{b}{2}} \qquad 83$$

Equations 73, 74, 82 and 83 may be rewritten with the unknown constants in the following order; A_o, B_1, B_2, C_2:

$$\text{Sin } k_o \frac{s}{2} A_o - e^{-jk_1 \frac{s}{2}} B_1 - e^{jk_1 \frac{s}{2}} B_2 + 0 = 0$$

$$-\frac{\omega\epsilon_o}{k_o} \text{Cos } k_o \frac{s}{2} A_o - \frac{\sigma_1}{k_1} e^{-jk_1 \frac{s}{2}} B_1 + \frac{\sigma_1}{k_1} e^{jk_1 \frac{s}{2}} B_2 + 0 = 0$$

$$0 + \frac{\sigma_1}{k_1} e^{-jk_1 \frac{b}{2}} B_1 - \frac{\sigma_1}{k_1} e^{jk_1 \frac{b}{2}} B_2 - \frac{\sigma_2}{k_2} e^{-jk_2 \frac{b}{2}} C_2 = 0$$

$$0 + e^{-jk_1 \frac{b}{2}} B_1 + e^{jk_1 \frac{b}{2}} B_2 - e^{-jk_2 \frac{b}{2}} C_2 = 0$$

In order to have nontrivial solutions, the determinant made up of the coefficients of the above homogeneous equations must be equal to zero. That is:

$$D = \begin{vmatrix} \sin k_o \frac{s}{2} & -e^{-jk_1 \frac{s}{2}} & -e^{jk_1 \frac{s}{2}} & 0 \\ -\omega \frac{\epsilon_o}{k_o} \cos k_o \frac{s}{2} & -\frac{\sigma_1}{k_1} e^{-jk_1 \frac{s}{2}} & \frac{\sigma_1}{k_1} e^{jk_1 \frac{s}{2}} & 0 \\ 0 & \frac{\sigma_1}{k_1} e^{-jk_1 \frac{b}{2}} & -\frac{\sigma_1}{k_1} e^{jk_1 \frac{b}{2}} & -\frac{\sigma_2}{k_2} e^{-jk_2 \frac{b}{2}} \\ 0 & e^{-jk_1 \frac{b}{2}} & e^{jk_1 \frac{b}{2}} & -e^{-jk_2 \frac{b}{2}} \end{vmatrix} = 0$$

Multiplying the fourth row of the above determinant by $-\frac{\sigma_2}{k_2}$ and adding to the third row, one has:

$$\begin{vmatrix} \sin \frac{k_o}{2} s & -e^{-jk_1 \frac{s}{2}} & -e^{-jk_1 \frac{s}{2}} & 0 \\ -\frac{\omega \epsilon_o}{k_o} \cos k_o \frac{s}{2} & -\frac{\sigma_1}{k_1} e^{-jk_1 \frac{s}{2}} & \frac{\sigma_1}{k_1} e^{jk_1 \frac{s}{2}} & 0 \\ 0 & (\frac{\sigma_1}{k_1} - \frac{\sigma_2}{k_2}) e^{-jk_1 \frac{b}{2}} & -(\frac{\sigma_1}{k_1} + \frac{\sigma_2}{k_2}) e^{jk_1 \frac{b}{2}} & 0 \\ 0 & e^{-jk_1 \frac{b}{2}} & e^{jk_1 \frac{b}{2}} & -e^{-jk_2 \frac{b}{2}} \end{vmatrix} = 0$$

The above determinant reduces to:

$$e^{-jk_2\frac{b}{2}}\begin{vmatrix} \sin k_o\frac{s}{2} & -e^{-jk_1\frac{s}{2}} & -e^{-jk_1\frac{s}{2}} \\ -\frac{\omega\varepsilon_o}{k_o}\cos k_o\frac{s}{2} & -\frac{\sigma_1}{k_1}e^{-jk_1\frac{s}{2}} & \frac{\sigma_1}{k_1}e^{jk_1\frac{s}{2}} \\ 0 & (\frac{\sigma_1}{k_1}-\frac{\sigma_2}{k_2})e^{-jk_1\frac{b}{2}} & -(\frac{\sigma_1}{k_1}+\frac{\sigma_2}{k_2})e^{jk_1\frac{b}{2}} \end{vmatrix} = 0$$

Since the operating frequency is finite, $e^{-jk_2\frac{b}{2}}$ cannot be equal to zero; then the determinant has to be equal to zero. That is:

$$\left\{\frac{\sigma_1}{k_1}\sin k_o\frac{s}{2}\left[\frac{\sigma_1}{k_1}\left(\frac{\sigma_1}{k_1}+\frac{\sigma_2}{k_2}\right)e^{j\frac{k_1}{2}(b-s)} - \frac{\sigma_1}{k_1}\left(\frac{\sigma_1}{k_1}-\frac{\sigma_2}{k_2}\right)e^{-j\frac{k_1}{2}(b-s)}\right]\right.$$

$$\left. + \frac{\omega\varepsilon_o}{k_o}\cos k_o\frac{s}{2}\left[\left(\frac{\sigma_1}{k_1}+\frac{\sigma_2}{k_2}\right)e^{j\frac{k_1}{2}(b-s)} + \left(\frac{\sigma_1}{k_1}-\frac{\sigma_2}{k_2}\right)e^{-j\frac{k_1}{2}(b-s)}\right]\right\} = 0 \quad 84$$

Let

$$\frac{\sigma_1}{k_1}+\frac{\sigma_2}{k_2} = N_1 \quad 85$$

$$\frac{\sigma_1}{k_1}-\frac{\sigma_2}{k_2} = N_2 \quad 86$$

Substitution of Equations 81, 85, and 86 into Equation 84 gives the following interesting result:

$$\frac{\sigma_1}{k_1}\sin k_o\frac{s}{2}\left[N_1 e^{jk_1 d} - N_2 e^{-jk_1 d}\right]$$

$$+ \frac{\omega\varepsilon_o}{k_o}\cos k_o\frac{s}{2}\left[N_1 e^{jk_1 d} + N_2 e^{-jk_1 d}\right] = 0$$

Dividing through by Cos $k_o \frac{s}{2}$ and rearranging,

$$\tan k_o \frac{s}{2} = - \frac{\omega \epsilon_o k_1}{k_o \sigma_1} \left[\frac{N_1 e^{jk_1 d} + N_2 e^{-jk_1 d}}{N_1 e^{jk_1 d} - N_2 e^{-jk_1 d}} \right] \qquad 87$$

Recalling that

$$k_o^2 = \Gamma^2 + \omega^2 \mu_o \epsilon_o ,$$

and since from the approximate analysis Γ^2 is expected to be near the value $(-\omega^2 \mu_o \epsilon_o)$ found for the ideal case, k_o should be very small and it is reasonable for a first order analysis to approximate the tangent by the angle in Equation 87. Then

$$k_o \frac{s}{2} k_o = -\omega \epsilon_o \frac{k_1}{\sigma_1} \left[\frac{N_1 e^{jk_1 d} + N_2 e^{-jk_1 d}}{N_1 e^{jk_1 d} - N_2 e^{-jk_1 d}} \right]$$

or

$$k_o^2 = - \frac{2\omega \epsilon_o k_1}{\sigma_1 s} \left[\frac{N_1 e^{jk_1 d} + N_2 e^{-jk_1 d}}{N_1 e^{jk_1 d} - N_2 e^{-jk_1 d}} \right]$$

Let $\omega^2 \mu_o \epsilon_o = k_o^2$.

Then:

$$\Gamma^2 = -k_o^2 - \frac{2\omega \epsilon_o k_1}{\sigma_1 s} \left[\frac{N_1 e^{jk_1 d} + N_2 e^{-jk_1 d}}{N_1 e^{jk_1 d} - N_2 e^{-jk_1 d}} \right]$$

After some minor rearrangement,

$$\Gamma^2 = -k_o^2 \left[1 + \frac{2k_1}{k_o \sigma_1 \eta_o s} \left(\frac{N_1 e^{jk_1 d} + N_2 e^{-jk_1 d}}{N_1 e^{jk_1 d} - N_2 e^{-jk_1 d}}\right)\right]$$

where $\eta_o = \frac{\mu_o}{\epsilon_o}$, wave impedance in free space.

Factoring out $N_1 e^{jk_1 d}$ in the second term of the above equation, and letting $\frac{N_2}{N_1} = R$,

$$\Gamma^2 = -k_o^2 \left[1 + \frac{2k_1}{k_o \sigma_1 \eta_o s} \left(\frac{1 + R e^{-j2k_1 d}}{1 - R e^{-j2k_1 d}}\right)\right] \qquad 88$$

Ratio R may be expressed in terms of strip line parameters as follows:

$$R = \frac{k_2 \sigma_1 - k_1 \sigma_2}{k_2 \sigma_1 + k_1 \sigma_2}$$

Recalling from Equations 63, 70 and 77 that

$$k_o^2 = \gamma^2 + \omega^2 \mu_o \epsilon_o,$$

$$k_1^2 = -j\omega\mu_1\sigma_1,$$

and $$k_2^2 = -j\omega\mu_2\sigma_2,$$

the above relation for R then can be written as

$$R = \frac{(j\omega\mu_2\sigma_2)^{1/2} \sigma_1 - (j\omega\mu_1\sigma_1)^{1/2} \sigma_2}{(j\omega\mu_2\sigma_2)^{1/2} \sigma_1 + (j\omega\mu_1\sigma_1)^{1/2} \sigma_2}$$

Factoring out $(j\omega\sigma_1\sigma_2)^{1/2}$ from the above equation,

$$R = \frac{(\sigma_1\mu_2)^{1/2} - (\sigma_2\mu_1)^{1/2}}{(\sigma_1\mu_2)^{1/2} + (\sigma_2\mu_1)^{1/2}}$$

or

$$R = \frac{1 - (\frac{\sigma_2\mu_1}{\sigma_1\mu_2})^{1/2}}{1 + (\frac{\sigma_2\mu_1}{\sigma_1\mu_2})^{1/2}} \qquad 89$$

Substituting Equation 89 into Equation 88 and taking the square root, the propagation constant of the electromagnetic wave in the strip line in terms of strip line parameters and magnetic film permeability becomes:

$$\Gamma = jk_o \left\{ 1 + \frac{2k_1}{k_o\sigma_1\eta_o s} \left[\frac{1 + \dfrac{1 - (\frac{\sigma_2\mu_1}{\sigma_1\mu_2})^{1/2}}{1 + (\frac{\sigma_2\mu_1}{\sigma_1\mu_2})^{1/2}} e^{-j2k_1 d}}{1 - \dfrac{1 - (\frac{\sigma_2\mu_1}{\sigma_1\mu_2})^{1/2}}{1 + (\frac{\sigma_2\mu_1}{\sigma_1\mu_2})^{1/2}} e^{-j2k_1 d}} \right] \right\}^{1/2} \qquad 90a$$

where

$k_o = \omega(\mu_o\epsilon_o)^{1/2}$

$k_1 = j(j\omega\mu_1\sigma_1)^{1/2}$

σ_1 = permalloy conductivity

σ_2 = conductivity of conducting material in medium 2

d = magnetic film thickness

η_o = 377 ohms

s = spacing between two parallel planes

μ_2 = permeability of conducting material in medium 2

μ_1 = magnetic film permeability obtained from Equations 49 and 50

Combination of Equation 49 and 50 gives

$$\mu_{r1} = \frac{\mu_1}{\mu_o}$$

or

$$\mu_{r1} = \frac{(\omega_o^2 - \omega^2)[(\frac{\gamma M}{\mu_o})^2 - \omega^2]}{[(\omega_o^2 - \omega^2)^2 + (\alpha\gamma\frac{M}{\mu_o}\omega)^2]} - j\frac{(\alpha\gamma\frac{M}{\mu_o}\omega)[(\frac{\gamma M}{\mu_o})^2 + \omega^2]}{[(\omega_o^2 - \omega^2)^2 + (\alpha\frac{\gamma M}{\mu_o}\omega)^2]} \qquad 90b$$

As a check of the previous assumption, using the film relative permeability given in Figure 3, the spacing s about 1 millimeter and the film conductivity of 0.5×10^7 mhos per meter, with frequency high enough, it can be shown that the second term of Equation 90 is small and Γ^2 is in the order of $-\omega^2\mu_o\epsilon_o$.

The evaluation of the reflection coefficient is beyond the scope of this work, but once the propagation constant is known, the reflection coefficient (17) can be solved for by using the relation coefficient for the input impedance

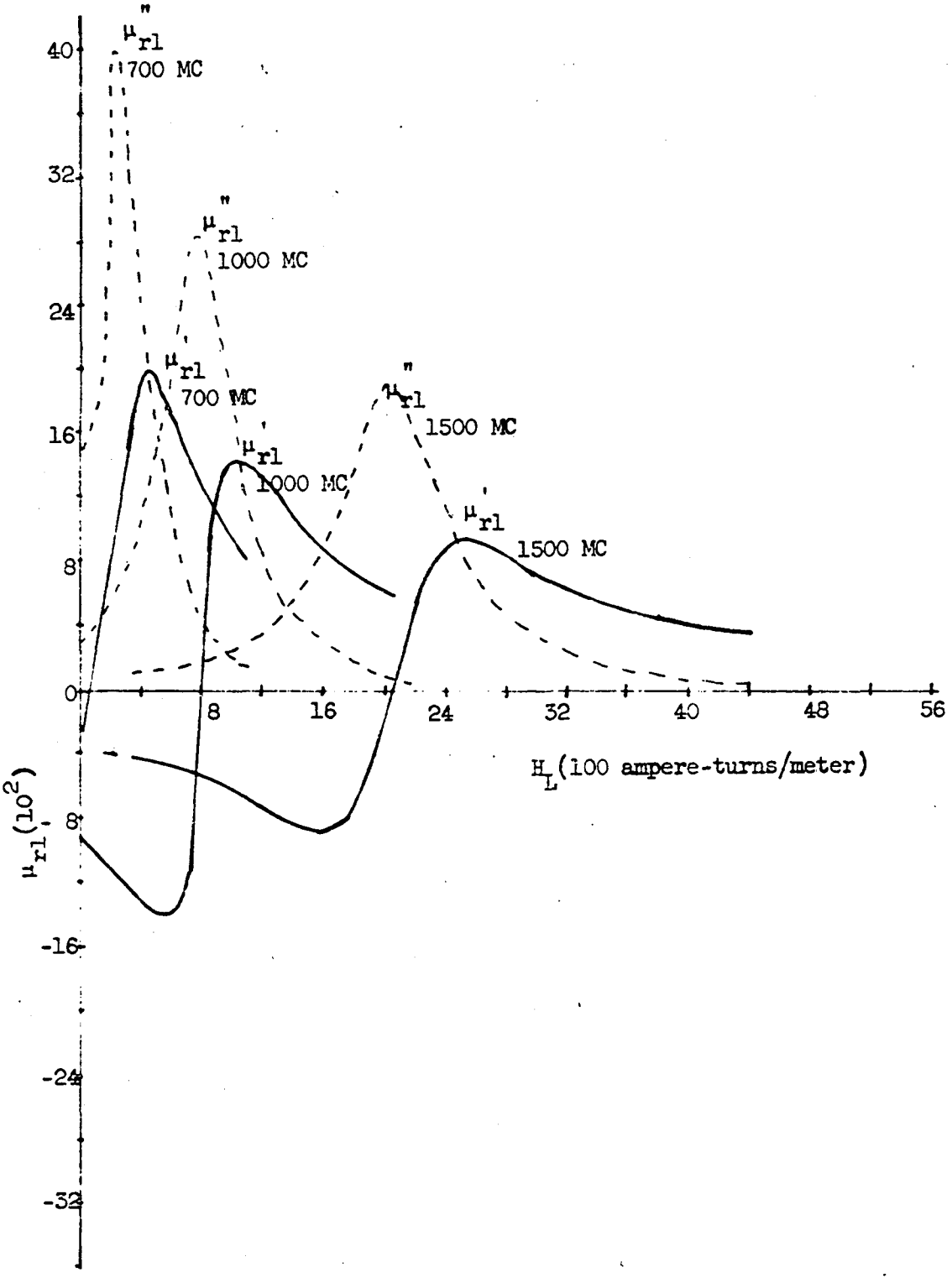

Figure 3. Film relative permeability components

$$z_i = \eta_c \left[\frac{z_L \cosh \Gamma \ell + \eta_c \sinh \Gamma \ell}{\eta_c \cosh \Gamma \ell + z_c \sinh \Gamma \ell}\right]$$

where η_c is the characteristic impedance

$$\eta_c = \frac{Ex^+}{Hy^+} = \frac{\frac{\Gamma}{k_o} A \cos k_o x}{j\frac{\omega\epsilon}{k_o} A \cos k_o x} = \frac{-j\Gamma}{\omega\epsilon_o}$$

The reflection coefficient is then:

$$\rho = \frac{z_i - z_L}{z_i + z_L}$$

4. Analytical evaluation of μ_{rl}, and the transmitted wave of electric field intensity

The Cyclone Computer was programmed to handle simultaneously Equations 90a and 90b, to give Re $\Gamma = \alpha$, Imag $\Gamma = \beta$, Re $\mu_{rl} = \mu'_{rl}$, and Imag $\mu_{rl} = \mu''_{rl}$. In addition, since α was found, the transmitted wave of electric field intensity through the length ℓ of the strip line was found in the same computer operation, the equation of the wave being $|E_{tr}| = 1.0\ e^{-\alpha\ell}$.

The parameters used for the computation are given below:

$a = 0.01$

$H_k = 240$ ampere-turns/meter

$s = 0.15 \times 10^{-3}$ meter

$d = 500$ A, 2000 A, 4000 A

$f = 700$ Mc, 1000 Mc, 1500 Mc, 2000 Mc

$\sigma_1 = 4.76 \times 10^6$ mhos/meter

$\sigma_2 = 6 \times 10^6$ mhos/meter

$M = 1$ weber/m^2

$\gamma = 2.21 \times 10^5$ cycles per second per ampere-turn per meter

H_L = variable bias field intensity, in ampere-turns per meter

a. Computation of film relative permeability, μ_{rl} The components of the relative permeability of the magnetic film are plotted in Figure 3 for three frequencies, 700 Mc, 1000 Mc and 1500 Mc. It is interesting to observe that the amplitude of the real part of the permeability is always half of that of the imaginary part, as predicted in Equation 53. The peak of the permeability curves decrease as a function of frequency and the half width of μ''_{rl} increases with frequency as predicted in Equations 52 and 53, respectively.

Another interesting feature is that the real part of the permeability beyond the resonance bias field intensity changes much more slowly than the imaginary part. Since the inductance is related to the real part of the permeability, one can then, by varying the bias field intensity, change the inductance from positive to negative and vice-versa.

The curves of both components shift to the left as frequency decreases, due to the presence of H_K of the film; at low frequency, one can expect the inductance will decrease as the field increases. One also notes that μ'_{rl} changes very fast between the positive and negative peaks. This behavior will be used in the device application as illustrated in Section III, B.

b. Computation of the attenuation constant, α With the results obtained from the computation, the curve of the real part of the propagation constant, i.e., the attenuation constant, was plotted vs. bias field intensity for 700 Mc, 1000 Mc and 1500 Mc for three different film thicknesses, 500A, 2000A, and 4000A as shown in Figures 4, 5, and 6.

It is observed that as frequency increases, the half width of the α curve also increases. The same effect is observed for the imaginary part of film relative permeability. An increase in frequency shifts the α curve toward the high bias field intensity and raises its amplitude by a small amount.

For d = 2000A, the half width increases and the peak of the α curve increases noticeably as frequency increases. It is also observed that the α curve is not symmetrical as one might expect from its similarity with the curve of the imaginary component of relative permeability. The slope on the right side of α curve is much sharper than that on the left.

For d = 4000A, similar behavior is observed. It is interesting to note that α changes more drastically with respect to frequency as the film becomes thicker and reaches an optimum thickness, approximately 3000 A in this study.

For film thickness of 2000A, as the frequency varies from 700 Mc to 1500 Mc, there is an increase in attenuation of 6.5 nepers per meter; while for a 500A film, there is only an increase of 2.0 nepers per meter for the same range of frequency.

c. Computation of the phase constant, β The solutions were obtained for β as a function of bias field intensity H_L for few typical frequencies

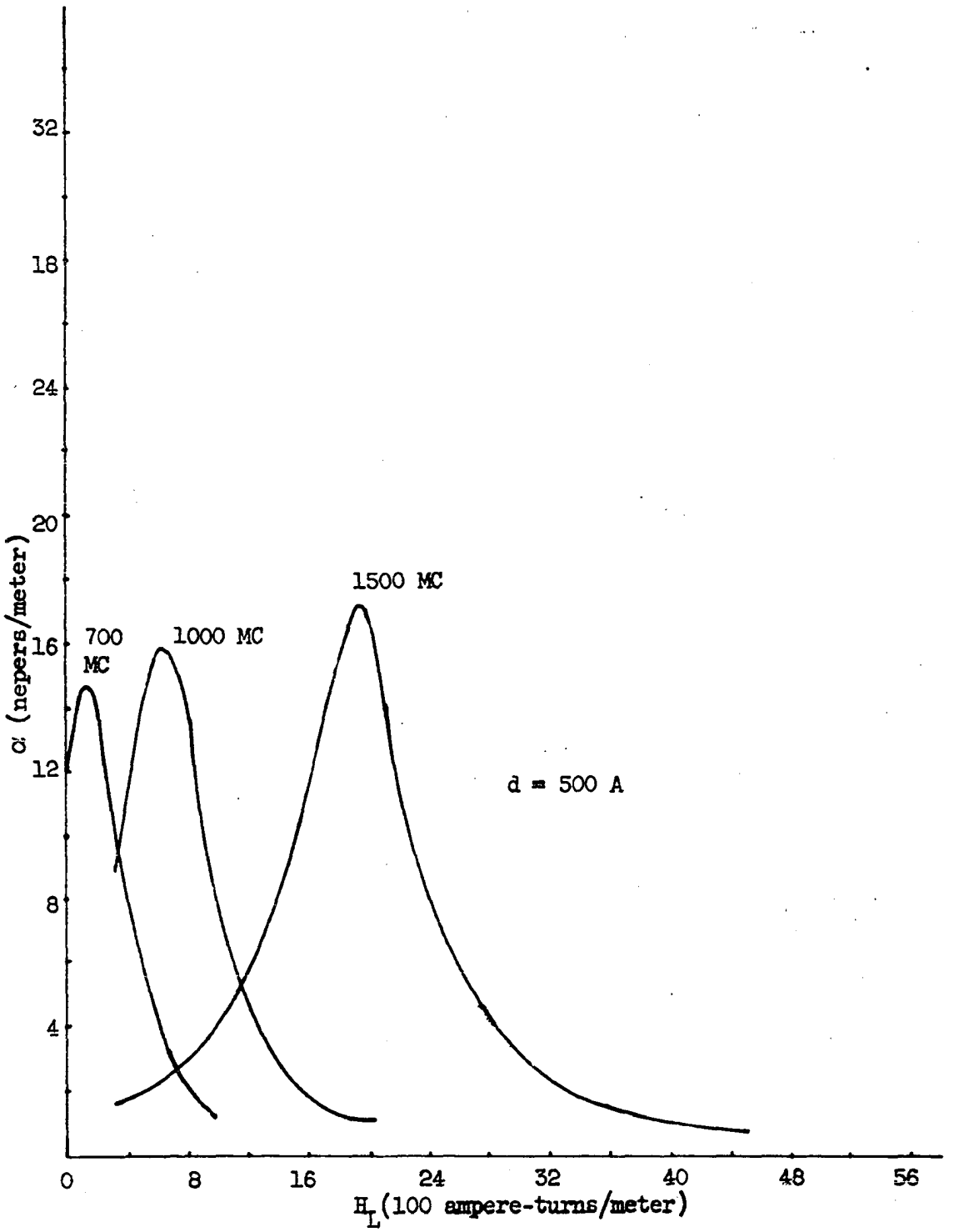

Figure 4. Attenuation constant

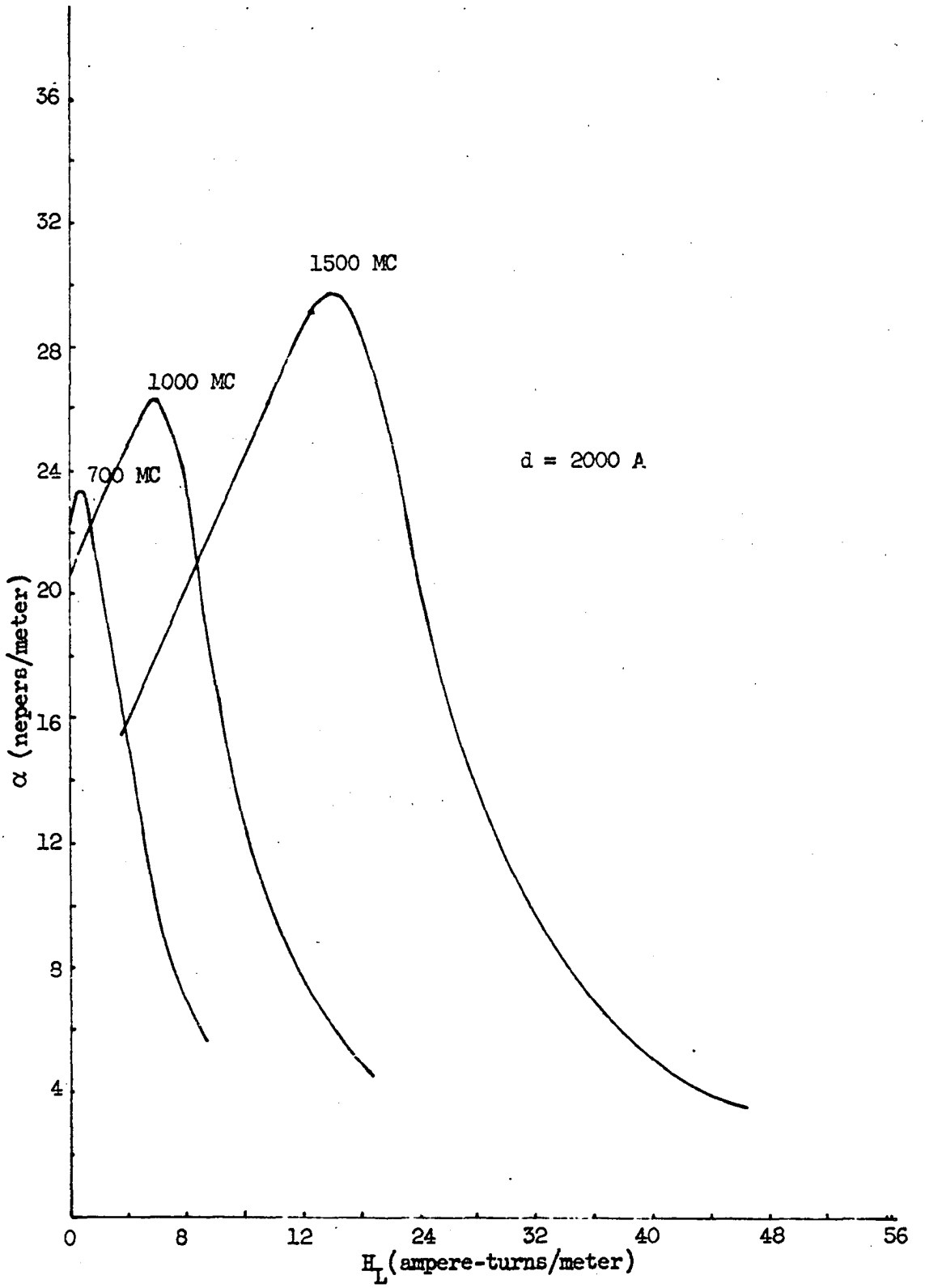

Figure 5. Attenuation constant

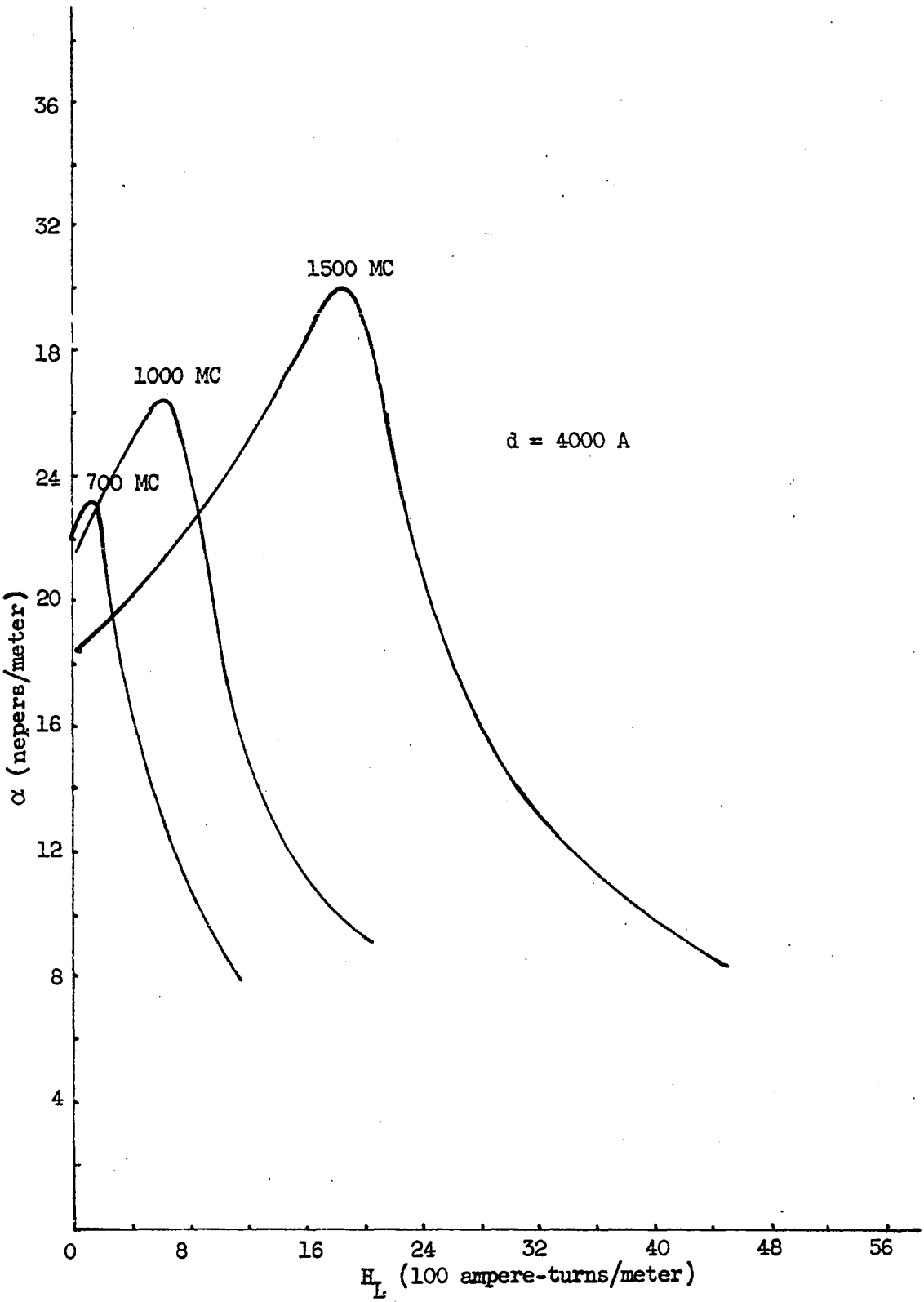

Figure 6. Attenuation constant

such as 700 Mc, 1000 Mc, 1500 Mc and 2000 Mc for certain film thicknesses. The curves of β for film thickness of 500A, 2000A and 4000A are shown in Figures 7, 8, and 9.

For d = 500A, one observes at all frequencies the β vs. H_L curves have the same shape as the μ'_{rl} curves shown in Figure 3. One might expect the difference between two peaks values of the curves to decrease as a function of frequency as does the difference between two peaks values of μ'_{rl}. On the contrary, the difference between the two peaks of β increases slightly, not at the same rate as that of μ'_{rl} decrease. The actual value of β does increase with frequency. One thing is true here for both the μ'_{rl} and β curves, that an increase in frequency does shift both curves toward the high field intensities as expected from the resonance Equation 32.

For d = 2000A, the phase angle β increases rapidly with H_L but the only curve which shows a distinct negative peak is that at 2000 Mc. For lower frequencies only the maximum of β is observed. The maximum phase difference for this thickness is about 31 radians per unit length.

For d = 4000A, a similar pattern is observed. Even though the β curve for 2000 Mc is not obtained, one may make the following observation:

> The difference between two peaks of the β vs. H_L curve does not increase much as function of frequency but does increase noticeably as the thickness increases. An increase in the film thickness has a tendency to shift the minimum of the curve toward the weak bias field intensity.

d. Computation of the transmitted wave In order to be able to compare the analytical result with the experimental result, it is desirable

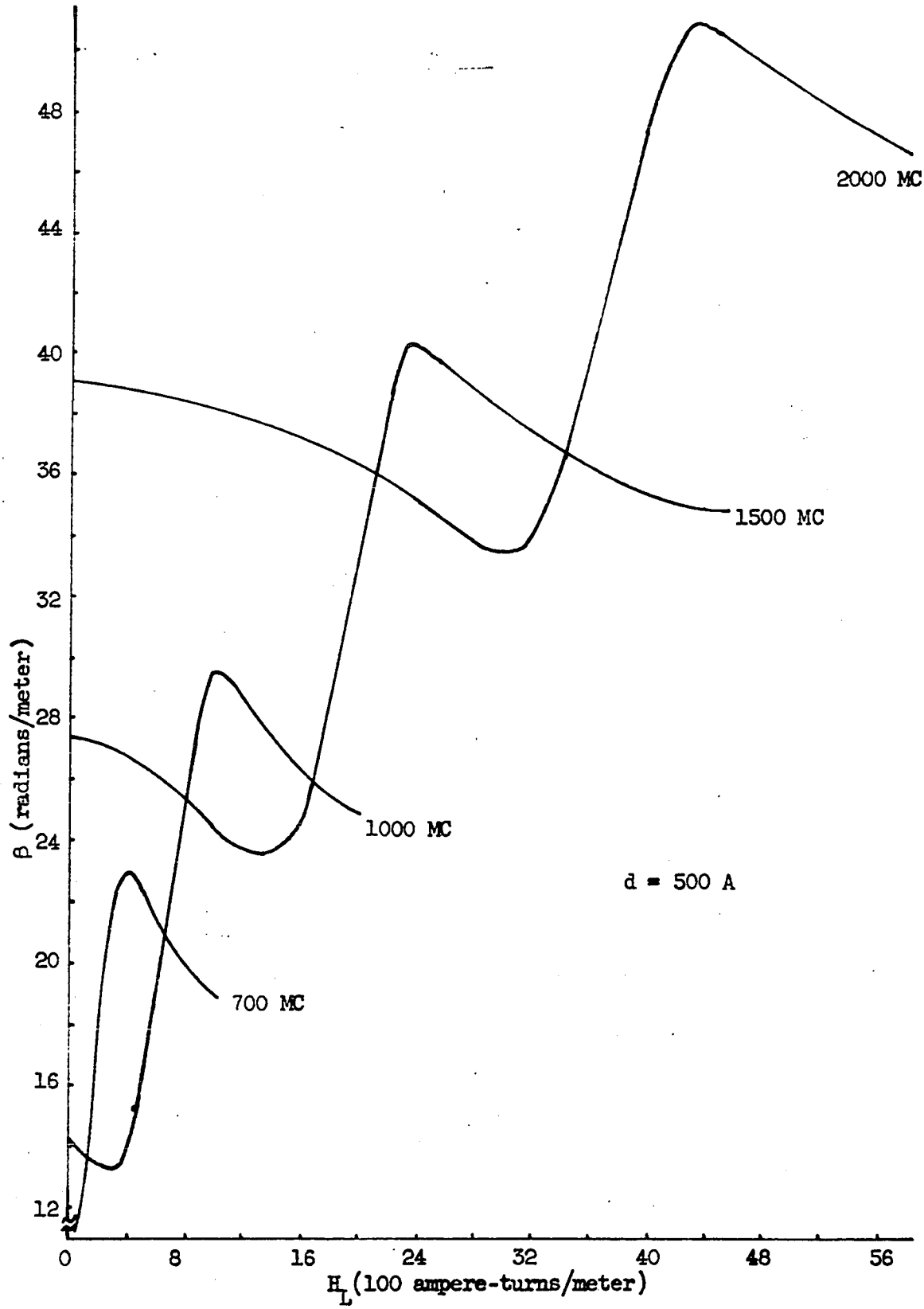

Figure 7. Phase constant

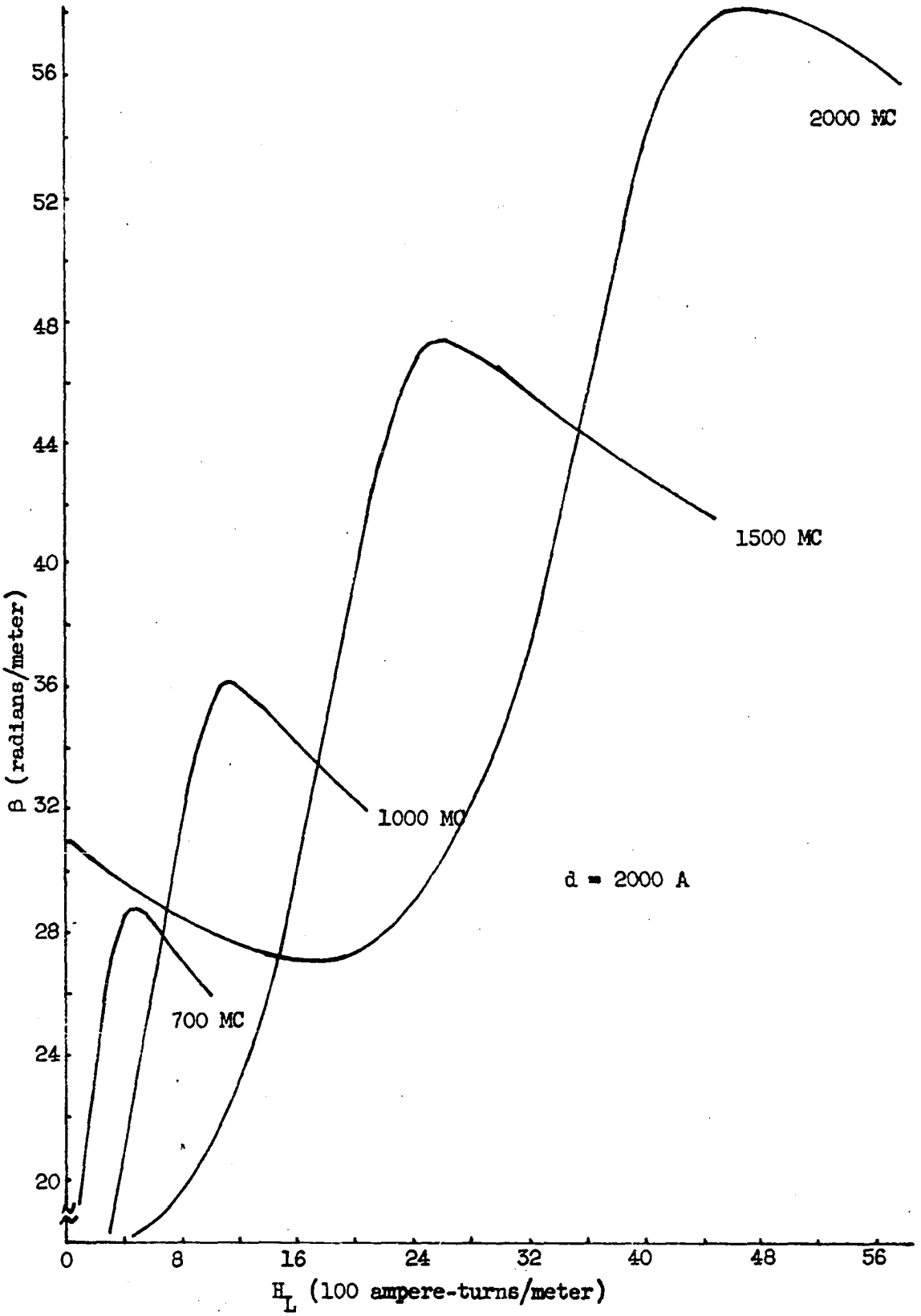

Figure 8. Phase constant

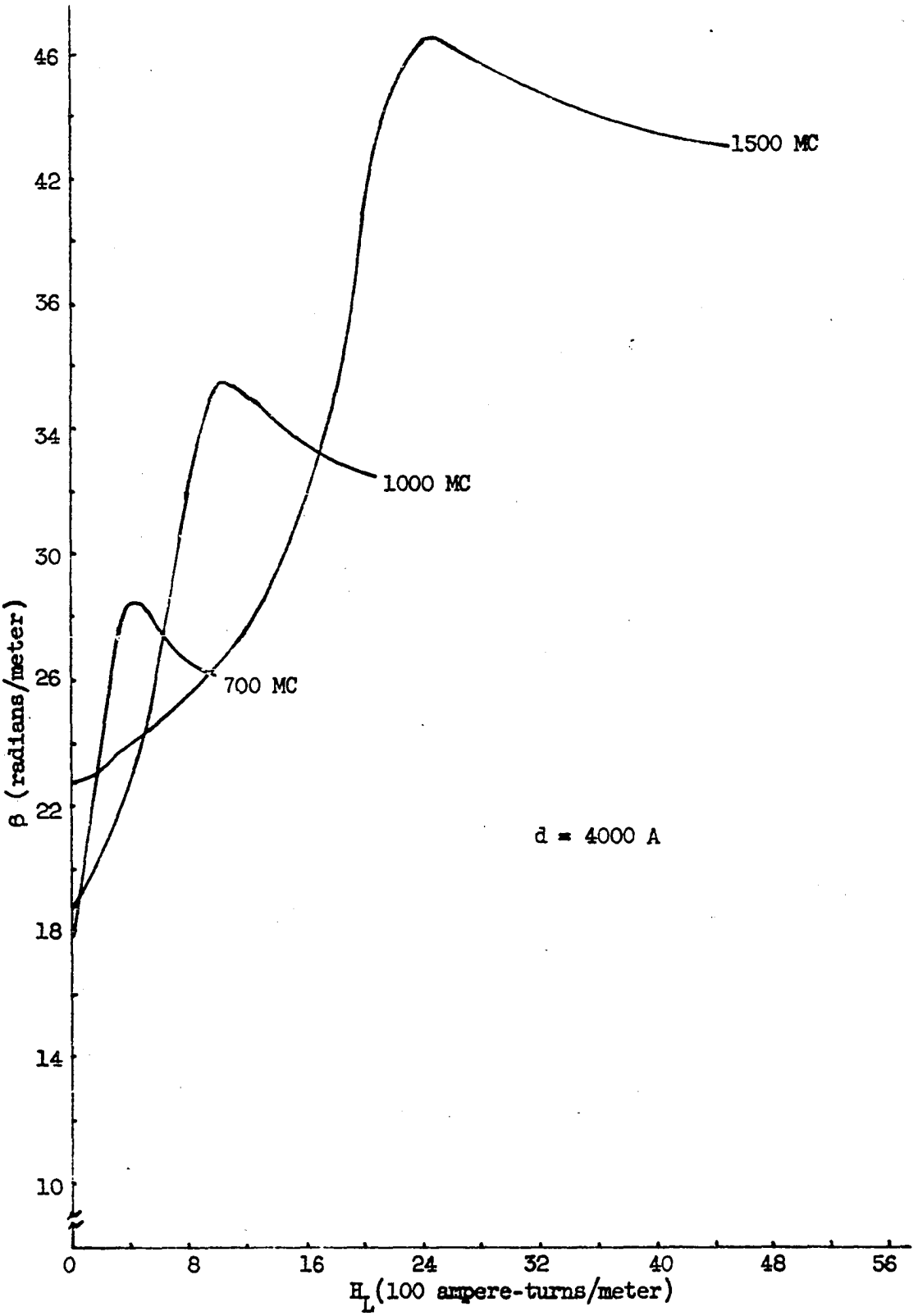

Figure 9. Phase constant

to use the proper length of the strip line considered in the experiment to formulate the transmitted wave. The length of the strip line used is approximately 0.06 meter.

Assuming that the electric field intensity at the input side of the strip line is maintained at unity, then the output electric field intensity can be expressed as

$$|E_{tr}| = 1.0\ e^{-\alpha(0.06)} .$$

The above equation is evaluated at 700 Mc, 1000 Mc and 1500 Mc for three different film thicknesses of 500A, 2000A and 4000A and the results are shown in Figures 10, 11, 12.

For d = 500A it is interesting to note that the amplitude of the transmitted wave, as a function of bias field intensity taken at different frequencies, has the form of the inverted attenuation curve. It is also observed that the amplitude of the transmitted wave decreases as the frequency increases and the half width increases with frequency.

For the geometry of the strip line in question, a film thickness of 500A can only suppress the amplitude of the transmitted wave down to one third for a certain frequency.

For d = 2000A, the half width increases with frequency and the minimum amplitude of the transmitted wave is half of that at 500A.

For d = 4000A, the same pattern is observed. It is of great interest to note that for this special thickness with the same bias condition and the same operating frequency, the amplitude of the transmitted wave is much less than for thinner films, and the minimum does not decrease

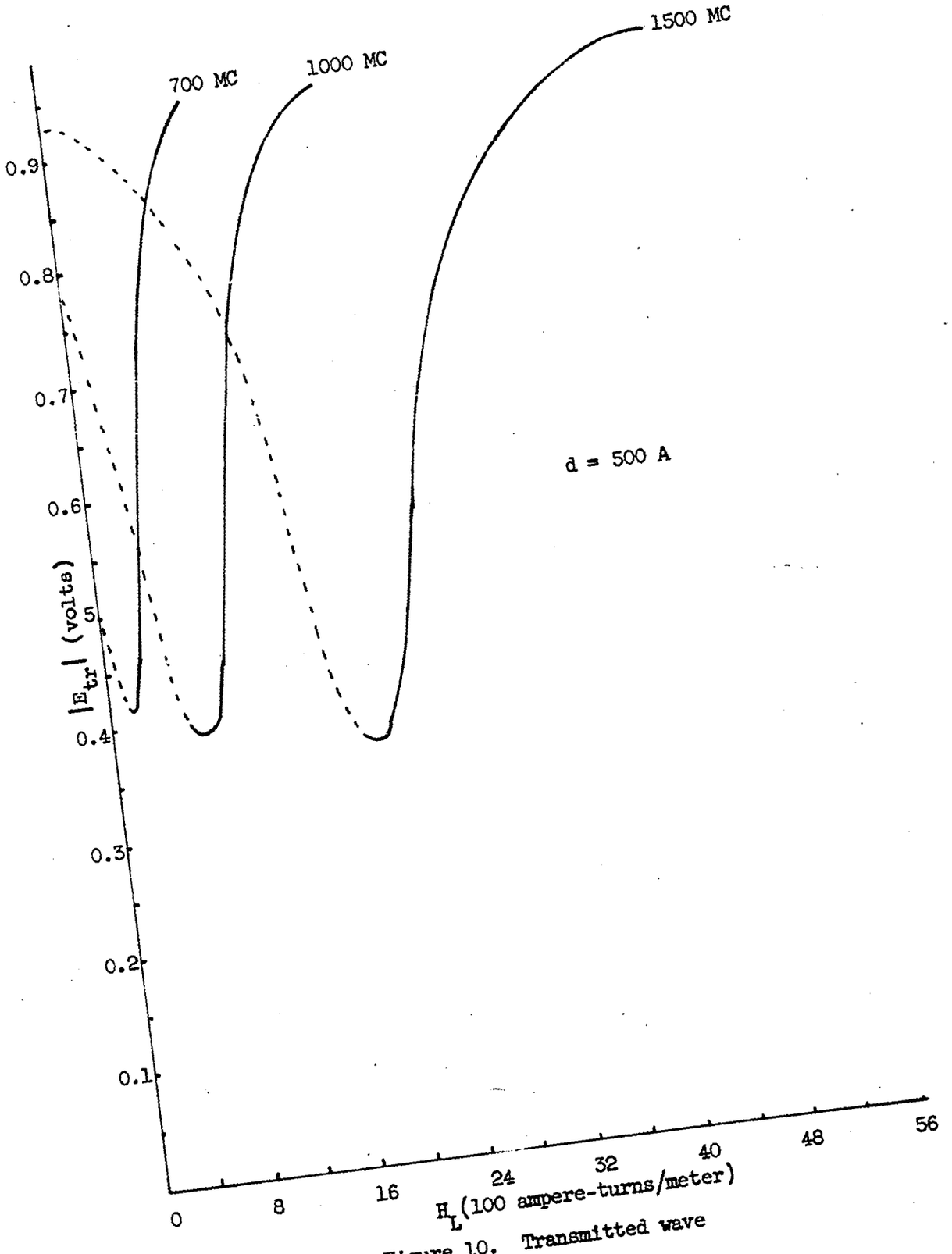

Figure 10. Transmitted wave

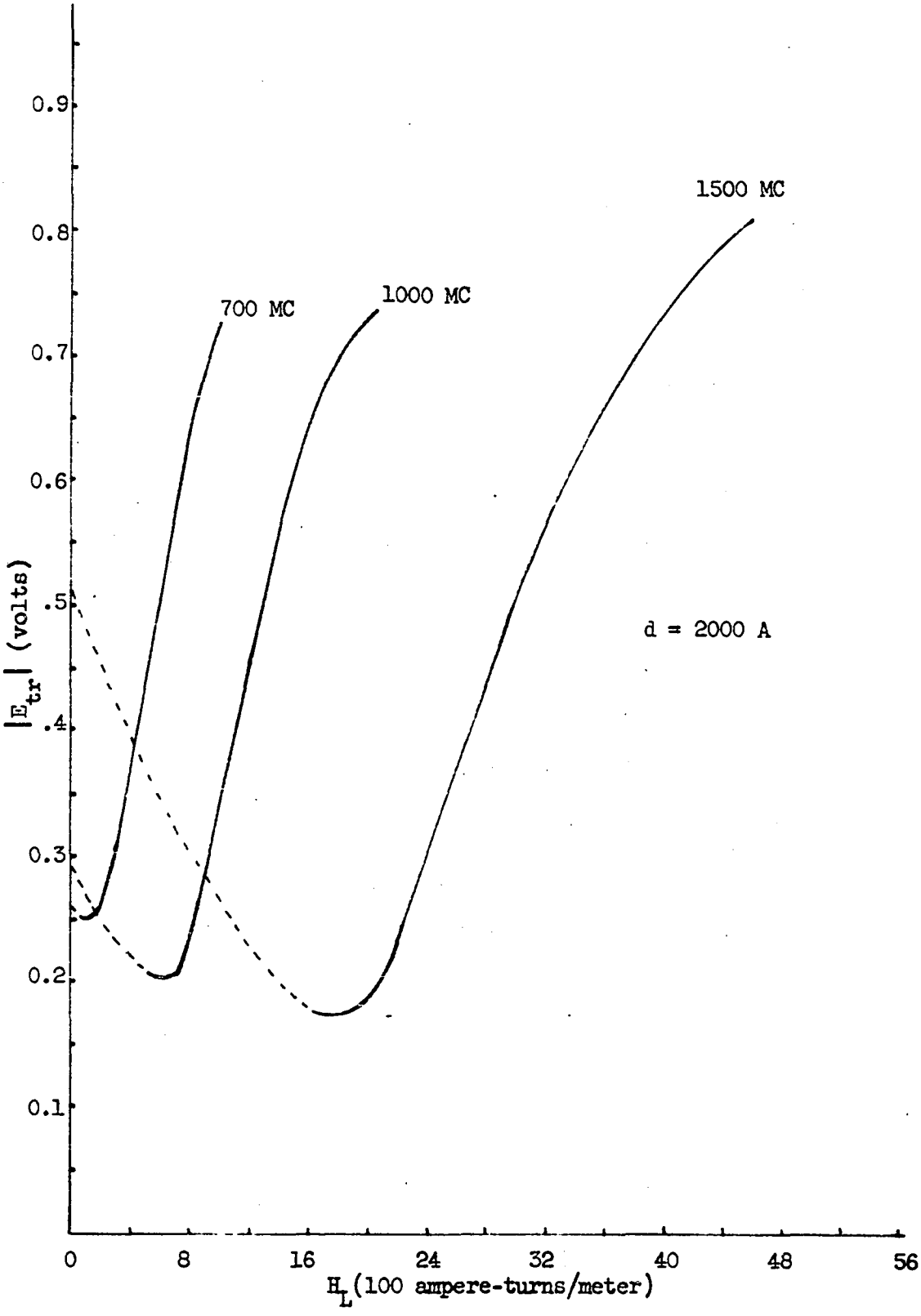

Figure 11. Transmitted wave

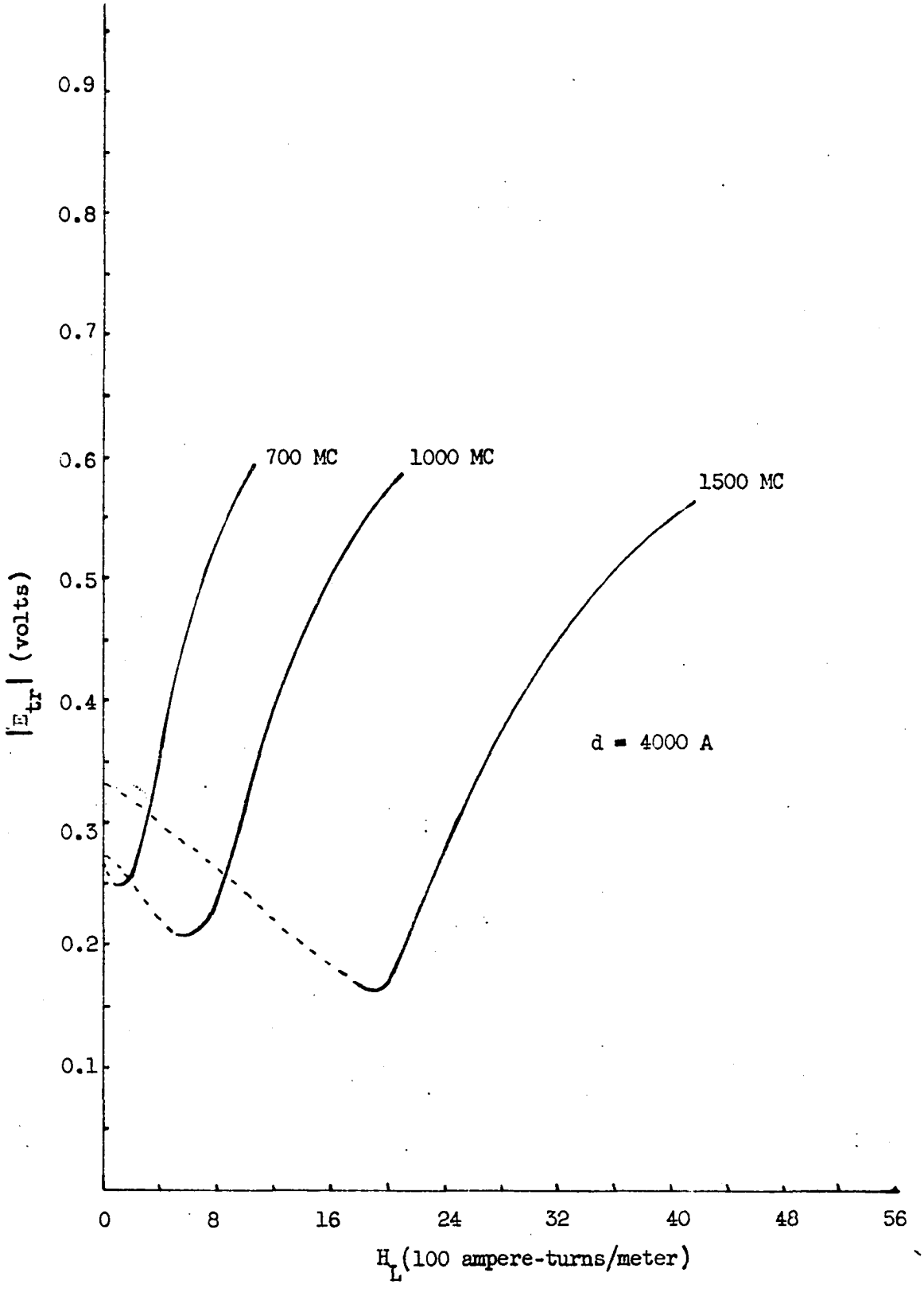

Figure 12. Transmitted wave

noticeably compared with that at 2000A.

Consequently it seems that an optimum film thickness will minimize the transmitted wave at the "cut-off" condition, i.e., at the lower peak of the transmitted wave, and give a fast rise of the wave amplitude in the transmitted region.

One can observe that the transmitted wave curves are almost symmetrical. The dashed parts of the curves are questionable. The points contributing to those parts of the curves were obtained with the assumption that the film was single domain and the rotation angle of the magnetization was small. These assumptions are no longer true at low bias field intensities. Theoretical investigation of this range of H_L is beyond the scope of this investigation.

B. Experimental Verification

1. Description of the strip line

The permalloy film was vacuum deposited on a 6 mil glass substrate 1 inch by 2 inches with the easy-direction along the width of the glass plate. The film was then cut into small strips 1 millimeter wide with the film easy-direction along the strip line. The film strips were then embedded on both sides of the center brass conductor of 3 mil thickness. The whole arrangement was then sandwiched between two outer grounded conductors made up of two pieces of brass 1 millimeter wide and 6 cm long. Figures 13 and 14 show the top and side views of the strip line used.

2. Measurements

The bias coil consisted of 800 turns wound around a square paper tube

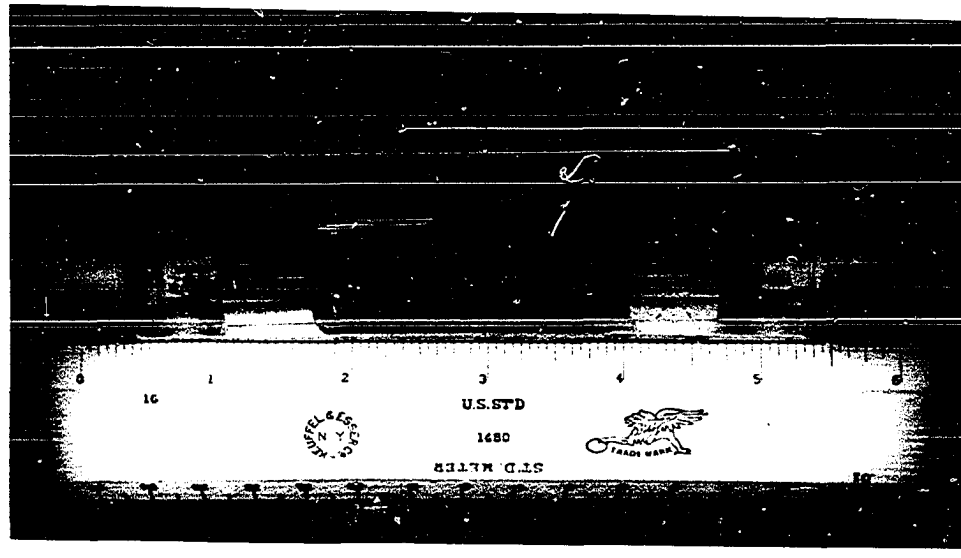

Figure 13. Top view of the strip line

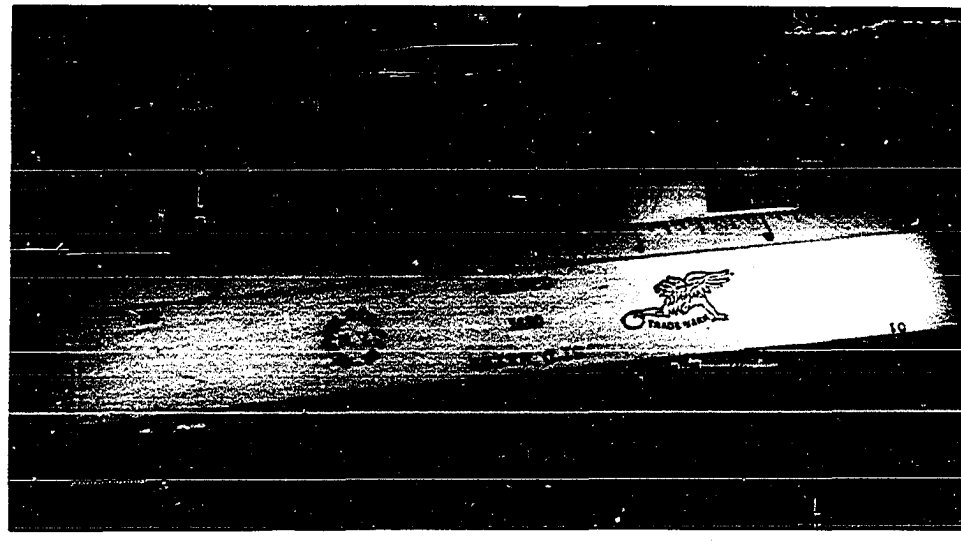

Figure 14. Side view of the strip line

with 1 square inch cross section and 6-1/2 inches long.

The measuring equipment consisted of:

Power oscillator, Type 124, Airborn Instruments Laboratory;

Variable attenuator, Type 874-GA, General Radio;

Coaxial slotted section, Type 805 A/B, Hewlett Packard;

Standing wave indicator, Type 415 B, Hewlett Packard;

Vacuum tube voltmeter, Model 610 B, Hewlett Packard;

Microwave power meter, Model 430 C, Hewlett Packard;

Power supply, Model 722 AR, Hewlett Packard.

Figure 15 gives the block diagram of the measurement set-up used in this investigation.

Due to the construction of the strip line and equipment limitations, the measurement of the phase constant could not be carried out as desired.

The transmitted power for a frequency range from 700 megacycles to 1250 megacycles was measured. An effort to maintain constant voltage across the strip line during the measurement was made with the available equipment. For the low frequency, the vacuum tube voltmeter was inserted between the strip line and the variable attenuator. Unfortunately this voltmeter can be operated only up to 700 megacycles. Above 700 megacycles the slotted line was used to locate the position of the strip line. The standing wave ratio meter was calibrated with the power meter, so the same power level could be maintained by observing the standing wave ratio meter indication throughout the measurements.

Before discussing the data, it is worthwhile to recall some differences between the analytical method and the experimental approach. In

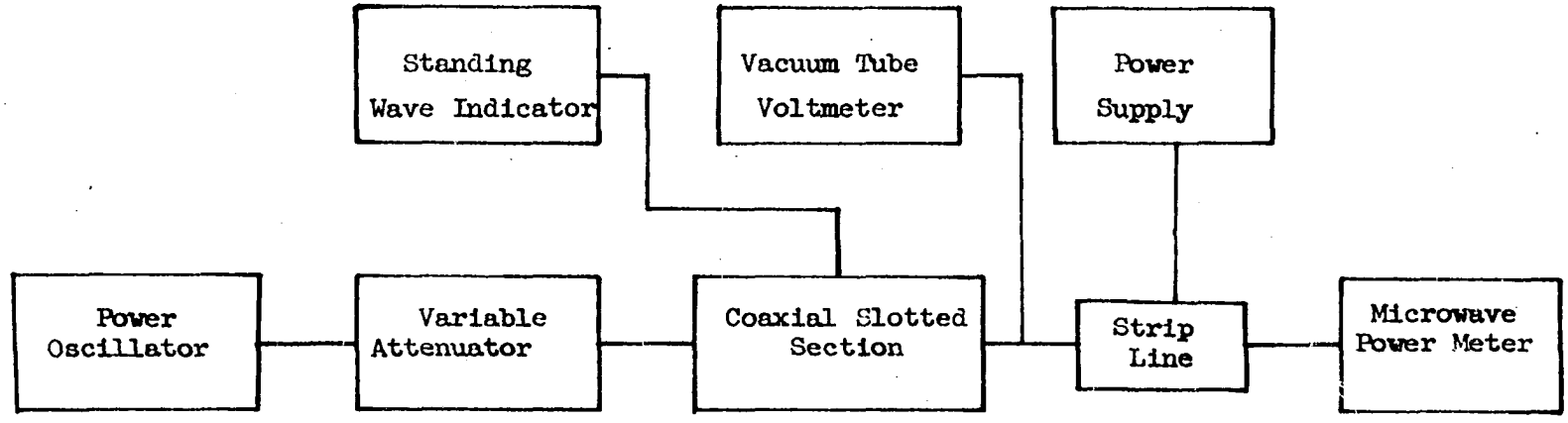

Figure 15. Diagram of microwave circuit used in investigation of the transmitted power and the voltage standing wave ratio

the analytical part, one evaluated the amplitude of the transmitted wave. In the experimental approach, the power of the transmitted wave was measured instead.

In order that the most general equations might be developed, the strip line considered in the analytical part was made up of two parallel plane conductors, both plated with permalloy, with air as the supporting dielectric. In the experimental work, since the minimum spacing between the two parallel plane conductors was desired, only one of the two planes was covered with permalloy film and glass was the supporting dielectric.

The data taken at 700 megacycles, 800 megacycles, 900 megacycles, 1000 megacycles and 1250 megacycles with the bias current varying from 0 to 1.2 amperes are presented in Figures 16 and 17.

C. Discussion

As pointed out previously, the strip line described in the analytical part and the model used for the experiment were not quite the same, due to the narrow choice of films and substrates. Hence the eddy current losses as well as the dominant effect of the film thickness are important reasons for the higher attenuation observed in the experimental results. In addition, the experimental output was measured in watts while the analytical output was computed in volts.

The irregular spacing between the output curves of Figure 16 is due to the switching of the voltage indicator at the strip line from the vacuum tube voltmeter to the slotted line and the standing wave indicator combination.

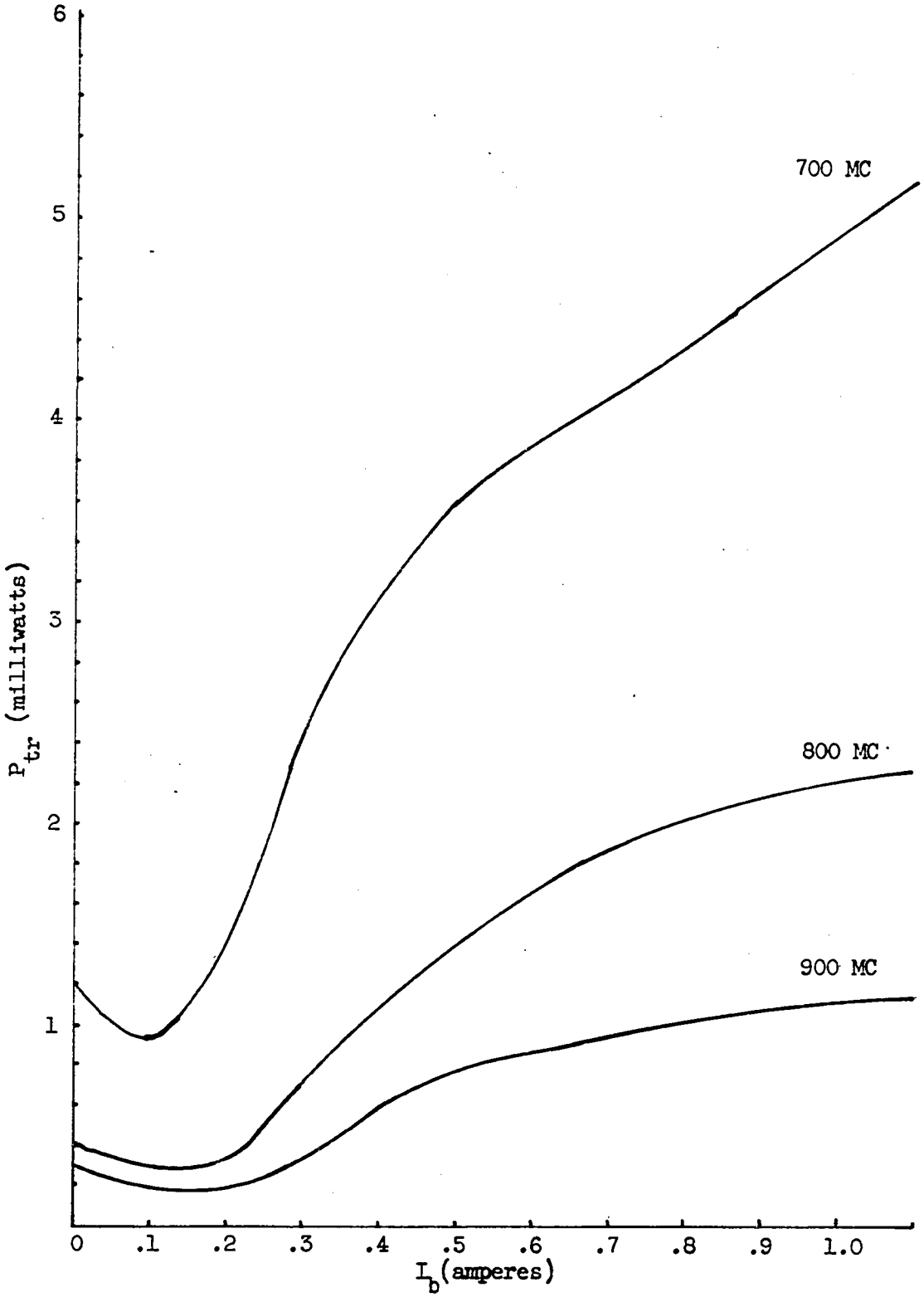

Figure 16. Transmitted power

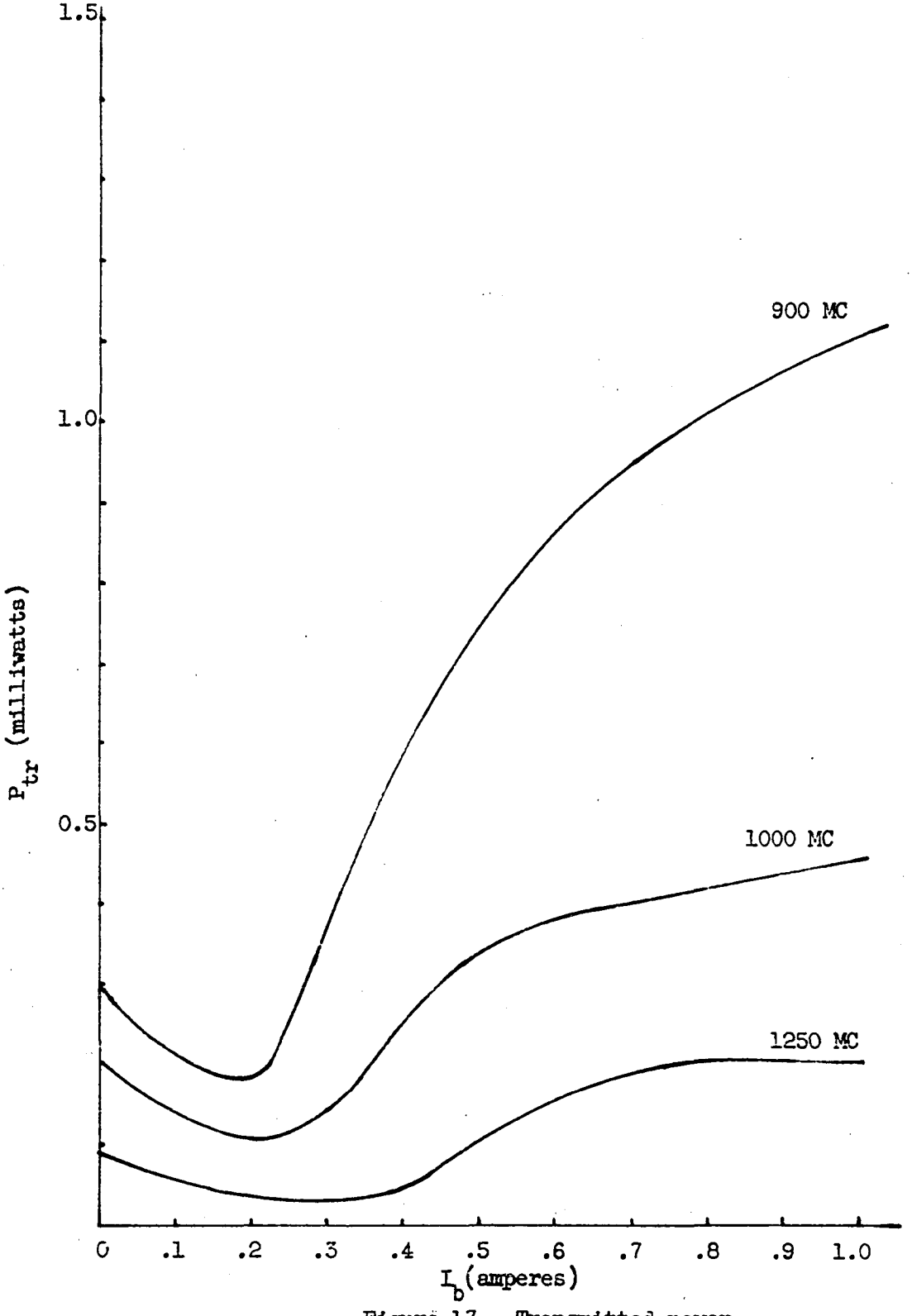

Figure 17. Transmitted power

It is interesting to note that at low bias field intensities, the experimental output curves do not cross one another as the analytical curves tend to show, because the latter were computed with the general assumption of a single domain film and a small angle of rotation.

The difficulty involved in the cutting of film into smaller strips may be alleviated by the use of electroplated wire as a center conductor. The strip line construction then reduces to a single task of putting the plated wire as a center conductor between two grounded planes (18).

Since the region of greater interest is near and beyond the resonance point, where the film is operated at high bias field intensity, film uniformity is secured and problems such as multidomain films or considerable low field loss at low bias field intensities are eliminated.

Another interesting observation may be made on the analytical results. If the transmitted wave amplitude curves of Figures 10, 11 and 12 are inverted and observed carefully, they bear some resemblance to the real part of the film permeability below resonance. In other words, the attenuation observed is not due mainly to the absorption curve and losses as one might expect, but also carries the earmarks of a reactive attenuation. The later phenomenon was verified experimentally by measuring the standing wave ratio, hence the reflection coefficient, as a function of bias field intensity. It was found that the standing wave ratio reached a maximum as the transmitted wave reached its "cut-off" and tapered down as shown in Figure 18 where both power transferred and the voltage standing wave ratio are plotted as function of bias field intensity at 700 Mc.

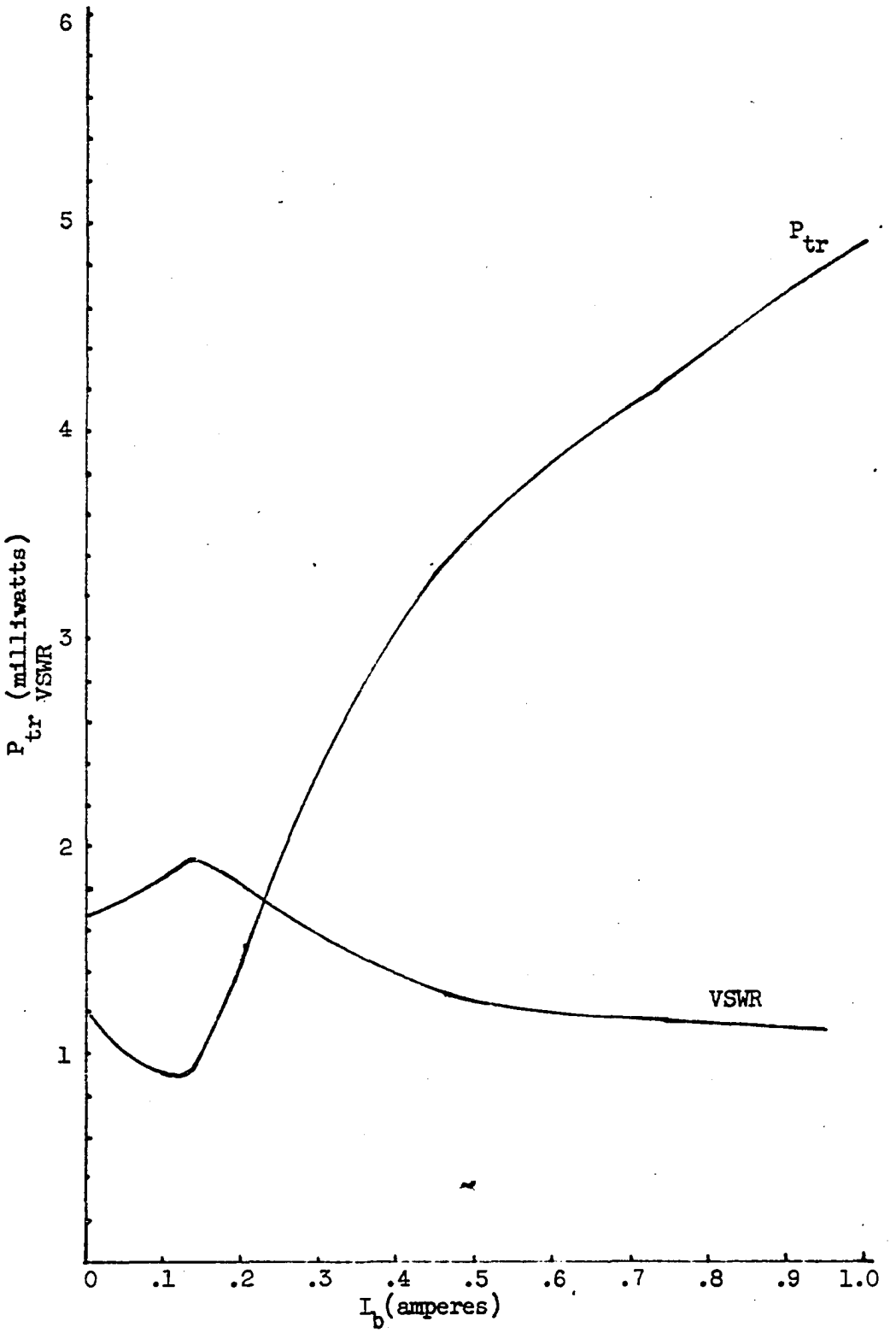

Figure 18. Transmitted power and voltage standing wave ratio (VSWR) at 700 MC

III. APPLICATIONS

A. A Technique To Determine the Phenomenological Damping Constant a, the Lande Splitting Factor g, and the Anisotropy Field Intensity H_K

It is interesting to note from Figure 7 that the phase difference between the minimum and the maximum does not change much with frequency but the half width does increase with frequency according to Equation 42.

$$\Delta H_L = \frac{a\omega}{\gamma} \qquad 42$$

where

$$\gamma = \frac{ge\,\mu_o}{2m}$$

As a consequence, one can expect that for certain film thickness, the losses do not affect the behavior of the β curves. Hence Equation 42 can be used to determine a or g for various frequencies. ΔH_L will be the arithmetic mean of the bias field intensities at the two peaks of the β curve.

As mentioned earlier, ferromagnetic resonance phenomena have been investigated (9 - 14). The phenomenological damping constant a, and the Lande splitting factor g, were determined by using the half width of the absorption curve measured by using cavity techniques. The absorption curve as obtained depends on the dispersion of the anisotropy field H_K. The above difficulty is eliminated by the method suggested above.

From data which can be obtained from Figure 7, one can also calculate H_K directly by using the resonance equation

$$\omega^2 = \gamma^2 \left[\frac{M}{\mu_o}(H_L + H_K)\right]$$

or

$$H_L = \frac{\omega^2 \mu_o}{\gamma^2 M} - H_K$$

Let H_{L1} be the bias field intensity necessary for resonant angular velocity ω_1 and H_{L2} be the bias field intensity necessary for resonant angular velocity ω_2.

Then

$$H_{L1} = \frac{\omega_1^2 \mu_o}{\gamma^2 M} - H_K$$

and

$$H_{L2} = \frac{\omega_2^2 \mu_o}{\gamma^2 M} - H_K$$

If the bias coil had a fixed number of turns per meter, then the ratio of the two equations above can be expressed in terms of the bias current as follows:

$$\frac{I_1}{I_2} = \frac{\frac{\omega_1^2 \mu_o}{\gamma^2 M} - H_K}{\frac{\omega_2^2 \mu_o}{\gamma^2 M} - H_K}$$

The above equation offers a method of determining H_K at any angular velocity by obtaining the curve for two different angular velocities and recording the corresponding bias currents.

3. Device Possibilities

1. A phase modulator

It is interesting to note from Figure 8, that for a film thickness of 2000A, at 2000 Mc, the maximum phase change is about 31 radians per unit length for a bias change of about 2900 ampere-turns/meter. Since the phase change is also a function of film thickness as seen from Figures 7 and 9, one can expect there is an optimum film thickness for a maximum phase change condition.

Referring to Equation 90a, the spacings between the two parallel planes is another parameter which can be used to advantage for this application. By reducing s, the phase constant β increases.

To obtain a certain phase constant, one can either increase the length of the strip line or reduce the spacing between two plane conductors.

Magnetic films are known for their high speed. The switching time is of the order of a nanosecond, hence the phase change as a result of applied bias field intensity can be expected to occur in the order of a relaxation time, i.e., in less than the usual switching time (19, 20).

2. An amplitude modulator

It is obvious from Figure 11, where the amplitude of the transmitted wave is plotted vs. the bias field intensity, an amplitude modulator at microwave frequency can be obtained. The normalized transmitted wave amplitude can be controlled to vary from 0.18 to 0.7 linearly as the bias field intensity sweeps from 2000 to 3700 ampere-turns per meter. Here again, the amplitude change will depend on the film thickness and the operating frequency. As in phase modulator applications, the parameter s in

Equation 90a can also be adjusted for the maximum advantage.

3. A thin film microwave switch

It has already been shown that at certain bias field intensities, a minimum transmitted power occurs; at other intensities, almost complete transmission occurs. This achieves the purpose of a microwave switch. Even though the magnetic film is not able to completely cut off the transmitting wave as seen in Figure 11, complete cut-off is not required in certain applications. If space limitation is a major problem, then the magnetic film geometry advantage can be used to fabricate compact miniature microwave switches. One can change from one state to the other as fast as the bias current can be switched, since it only takes the film less than a nanosecond to change from one state to the other.

4. A tunable low pass filter

From the resonance relationship

$$\omega_o^2 = \gamma^2 \frac{M}{\mu_o}(H_L + H_K) \qquad 32$$

and Figures 16 and 17, one can expect for a specific bias cut-off to occur at a specific ω_1. Waves at angular velocities below ω_1 will be transmitted, while those at angular velocities above ω_1 will be suppressed.

It is interesting to note that one can tune to any cut-off frequency just by applying the proper bias. The disadvantage is that the strip line cannot cut off the wave completely, but in cases where complete cut-off is not an important factor but space-saving and speed are mostly desired then the magnetic film can be of advantage.

5. An electrically movable discontinuity in the strip line

In a transmission line, it is often desirable for matching or tuning purpose to be able to move the short along the line. As pointed out in Section II, C the cut-off occurs as a result of reactive attenuation, hence reflection occurs at cut-off as indicated by the maximum VSWR recorded at cut-off bias. The film biased for cut-off can be considered as a discontinuity in the strip line.

Let H_o be the bias field intensity necessary for the discontinuity to occur. If the strip line was located along the x-axis and if the bias coil was wound such that the magnetic field intensity decreases linearly as a function of x, then by varying the bias current one can electrically move the discontinuity to any point x_1, x_2, x_3 anywhere along the strip line, as pictured in Figure 19.

The above solenoid has been designed and checked. It is found out that in order for the magnetic field intensity to decrease linearly as a function of position, the number of ampere-turns per meter on the solenoid is inversely proportional to x.

6. A uniform OR circuit at microwave frequency

It is very difficult to make a large film matrix uniform by either evaporation or electroplating. Since the dots comprising the matrix are not uniform, some are single domain and others are not; as a result, the signal induced at low field intensities will be non uniform.

High field intensities will force all films to be single domain; as a result, the induced voltages will be identical. If the bias coil of the strip line is made up of a number of uniform coils, then a finite bias

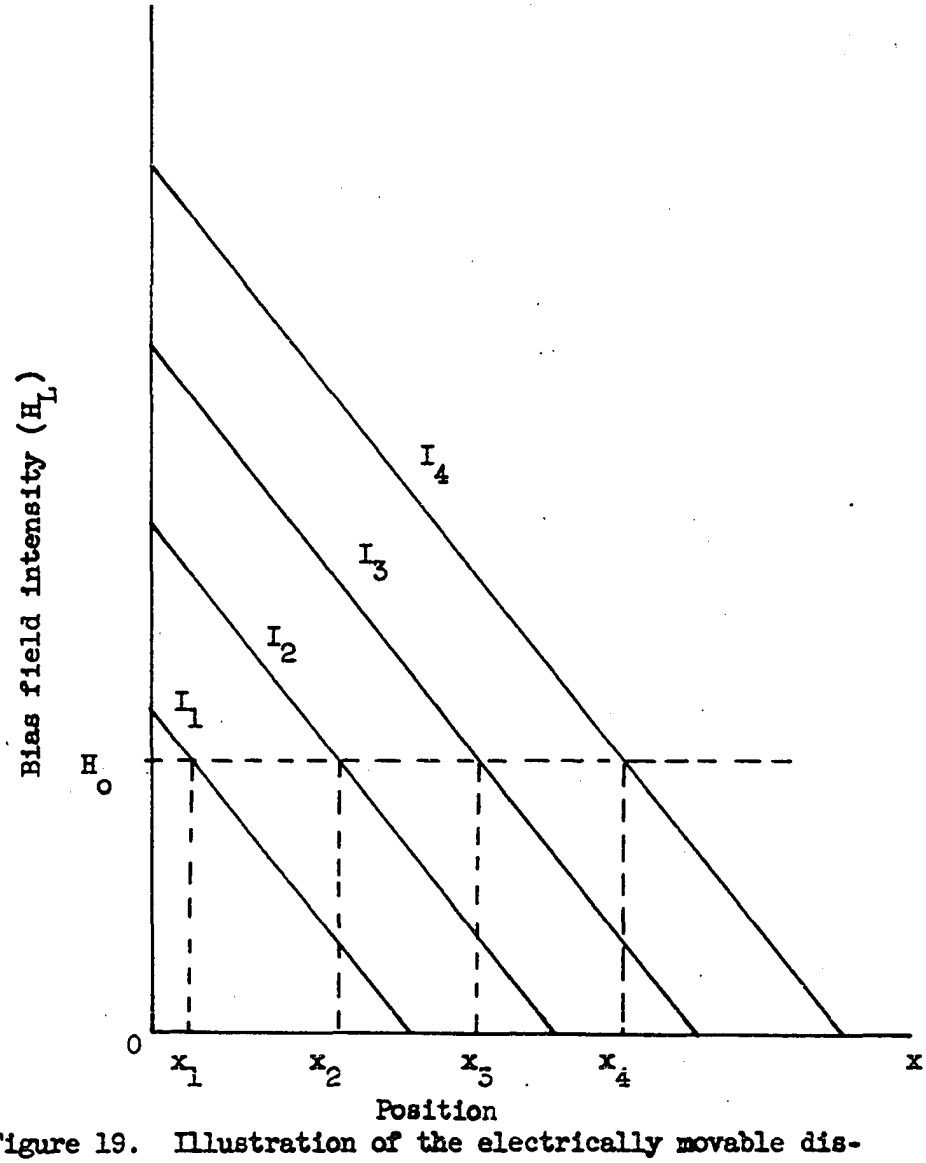

Figure 19. Illustration of the electrically movable discontinuity

current applied to any coil will yield a fixed output at the end of the strip line. As a result one has a uniform OR circuit.

The devices suggested in this section, as the title of the section implies, are only device possibilities. Some special design will be necessary in each case in order that the application conditions imposed may be met.

Naturally there are other device possibilities that could result from the above strip line or any modification of it. No attempt has been made to cover all of them in this work. Only a few typical possibilities have been mentioned.

IV. SUMMARY

Magnetic films with their flexible geometry and attractive magnetic properties are of increasing interest in the area of electrical devices. The purpose of this work was to investigate at microwave frequencies, the discontinuity caused by a variably biased magnetic film in a strip line and as a result to point out some typical applications.

The strip line under mathematical investigation consisted of two parallel conducting planes in contact with two permalloy films of variable thickness from 500 angstroms to 4000 angstroms, separated by air. The "easy direction" of the magnetic film was along the length of the strip line. An electromagnetic wave was propagated along the strip line. The expression for the propagation constant was developed, with boundary conditions imposed by the three layers with their respective permeabilities, dielectric constants and conductivities. The only significant variable with the bias was the permeability of the permalloy film.

The permeability of the magnetic film was obtained by simultaneous solution of the Landau-Lifshitz equation and Maxwell's wave equations, with the assumption of a small rotation angle at high bias field intensities. The half-width of the relative permeability curve and the relative peak values of the real and imaginary components of the complex permeability were determined.

The Cyclone Computer was programmed to solve for the complex relative permeability of the magnetic film, the attenuation constant and the phase constant of the strip line, and the magnitude of the transmitted electric field intensity. Suitable curves of the above quantities were plotted.

The following observations are of importance:

(1) a cut-off condition exists, at which the transmitted field intensity is suppressed to a minimum due to the reactive attenuation caused by the variable permeability of the film;

(2) per unit length of strip line, the phase constant changes by approximately 30 radians and the transmitted field intensity varies by approximately 80 percent as the bias field intensity varies from 1600 to 4500 ampere-turns per meter;

(3) the phase constant curves are similar in form to those of the real part of the relative permeability;

(4) high bias field intensity "forces" the magnetic film to be single domain;

(5) the phenomenological damping constant, the Lande splitting factor and the anisotropic field intensity may be determined by applying the half width equation to the phase constant curve.

Some typical devices at microwave frequency were suggested, including a phase modulator, an amplitude modulator, a microwave switch, a tunable low-pass filter, an electrically movable discontinuity and certain logic circuits.

An experimental model of the strip line was built. Measurements of the output power and the voltage standing wave ratio agreed quite well with predicted results at high bias field intensities.

V. LITERATURE CITED

1. Wolf, I. W., Katz, H. W., and Brain, A. E. The fabrication and properties of memory elements using electrodeposited thin magnetic films of 82-12 nickel-iron. Electronic Components Conference Proceedings; 1959: 15-20. 1959.

2. Long, T. R. Electrodeposited memory element for a nondestruction memory. J. Appl. Phys. Suppl., 31: 123S-124S. 1960.

3. Kittel, C. and Galt, J. K. Ferromagnetic domain theory. In Seitz, F. and Turnbull, D., eds. Solid state physics. Vol. 3. pp. 437-557. New York, N. Y., Academic Press. 1956.

4. Kittel, C. Introduction to solid state physics. 2nd ed. New York, N. Y., John Wiley and Sons, Inc. 1956.

5. Kittel, C. Physical theory of ferromagnetic domain. Rev. Mod. Phys. 21: 541-583. 1949.

6. Decker, A. J. Solid state physics. Englewood Cliffs, N. J., Prentice-Hall, Inc. 1957.

7. Landau, L. and Lifshitz, E. On the theory of dispersion of magnetic permeability in ferromagnetic bodies. Physik Zeitschrift Sowjetunion. 8: 153-169. 1955.

8. Kittel, C. On the theory of ferromagnetic resonance absorption. Phys. Rev. 73: 155-161. 1948.

9. Turner, E. H. and Lee, J. B. Ferromagnetic resonance in thin magnetic film at radio frequency. J. Appl. Phys. 32: 1807-1810. 1961.

10. Conger, R. L. and Essig, F. C. Resonance and reversal phenomena. Phys. Rev. 104: 915-923. 1956.

11. Kingston, R. H. and Tannenwald, P. E. Ferromagnetic resonance at uhf in thin film. J. Appl. Phys. 29: 232-233. 1958.

12. Smith, D. O. Static and dynamic behaviour of thin permalloy film. J. Appl. Phys. 29: 264-273. 1958.

13. Rado, G. T. Ferromagnetic phenomena at microwave frequency. Advances in electronics. Vol. 2. New York, N. Y., Academic Press, Inc. 1950.

14. Bozworth, R. M. Ferromagnetism. New York, N. Y., D. Van Nostrand Co., Inc. 1951.

15. McDonald, J. R. Spin exchange effects in ferromagnetic resonance. Phys. Rev. 103: 280-286. 1956.

16. Amen, W. S. and Rado, G. T. Electromagnetic effects on spin wave resonance in ferromagnetic materials. Phys. Rev. 97: 1558-1566. 1955.

17. Ramo, S. and Whinnery, J. R. Fields and wave in modern radio. 2nd ed. New York, N. Y., John Wiley and Sons, Inc. 1958.

18. Wholey, W. B. and Eldred, W. N. A new type of slotted line section. Institute of Radio Engineers Proceedings 38: 244-248. 1950.

19. Smith, D. O. Magnetization reversal and thin film. J. Appl. Phys. 29: 264-273. 1958.

20. Olson, C. D. and Pohm, A. V. Flux reversal in thin films of 82% Ni, 18% Fc. J. Appl. Phys. 29: 274-282. 1958.

VI. ACKNOWLEDGEMENTS

The writer wishes to take this opportunity to acknowledge the debt of gratitude to many persons who made this dissertation possible: to Dr. A. V. Pohm for his suggestions leading to this work and for his guidance and encouragement; to Professor W. L. Cassell for his counselling and for his many, many hours of help in preparation and suggestions for improvement in this dissertation; to his wife who stood by him in the many years of schooling and helped in the preparation of this dissertation; to Dr. M. S. Ulstad for his help in programming the Cyclone; to Professor B. S. Willis for taking pictures of the strip line. The help of Mrs. Sally Zembsch in the final preparation of this thesis is most gratefully acknowledged.